RadPath: Occipital Bone

Andrew Hill, MD
Gabriel Griffin, MD

Why the Occipital Bone?

- The temporal bone gets all the love when it comes to skull base
- The occipital bone is an important part of the craniovertebral junction (CVJ)
- Occipital bone lesions are often insidious in their growth and presentation

Objectives

- Review the embryology and anatomy of the occipital bone
- Review 2 synchondroses of the posterior skull base
  - Petro-occipital
  - Spheno-occipital
- Understand classic important differential diagnoses based on 2 locations:
  - Jugular Foramen
  - Clivus

Occipital Bone Anatomy

- Composed of:
  1. Basioccipital
  2. Exoccipital
  3. Supraoccipital

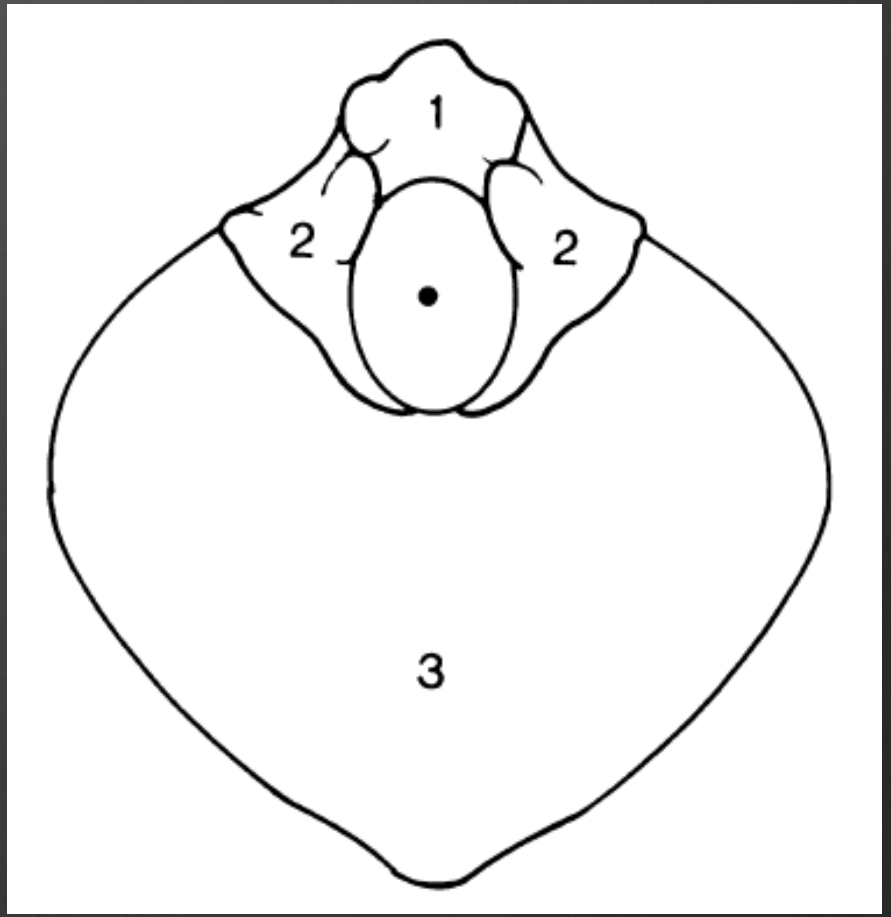

Sclerotomes

Majority of the Occipital Bone is derived from 4 occipital "sclerotomes"

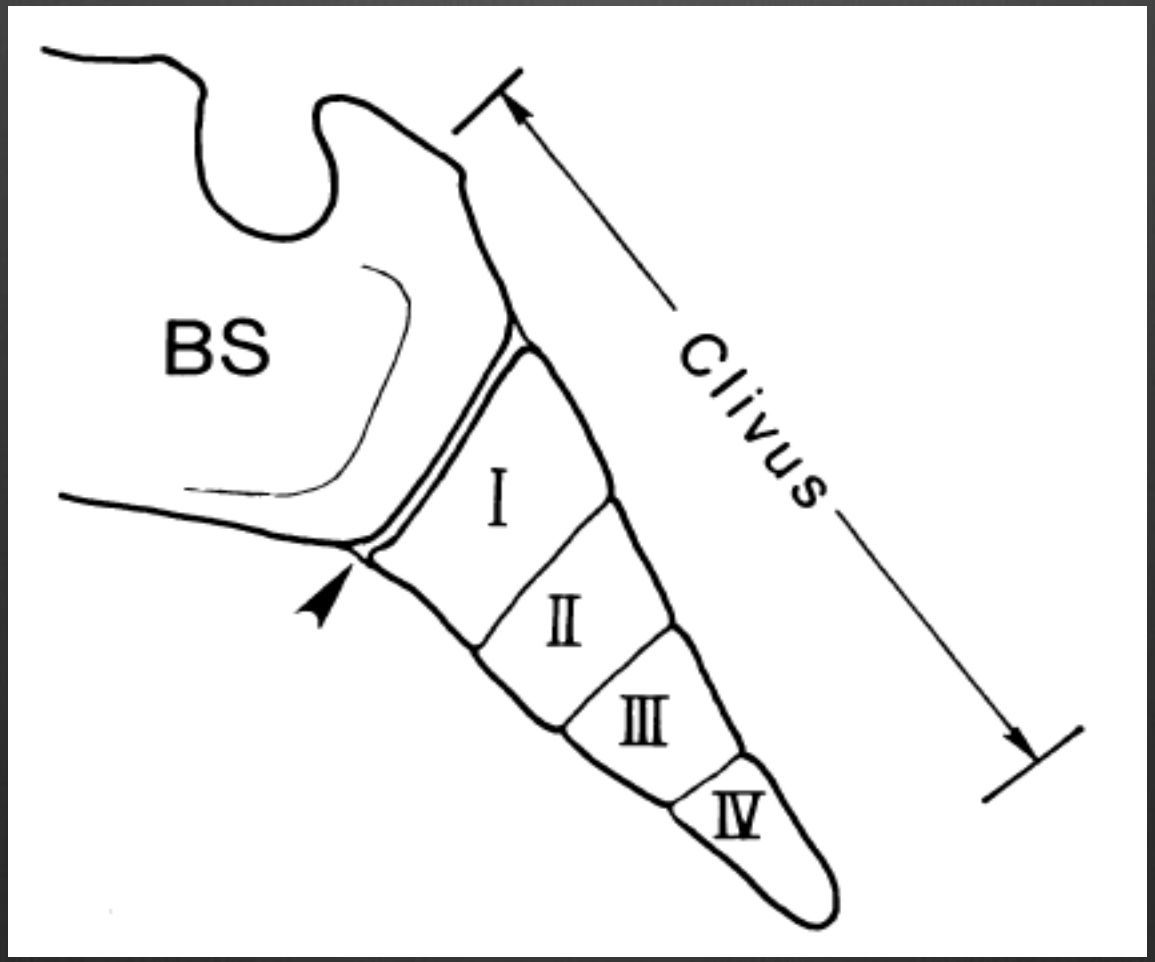

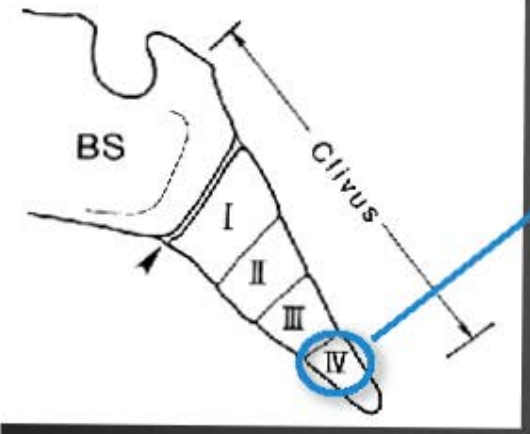
BS
Clivus
I
II
III
IV

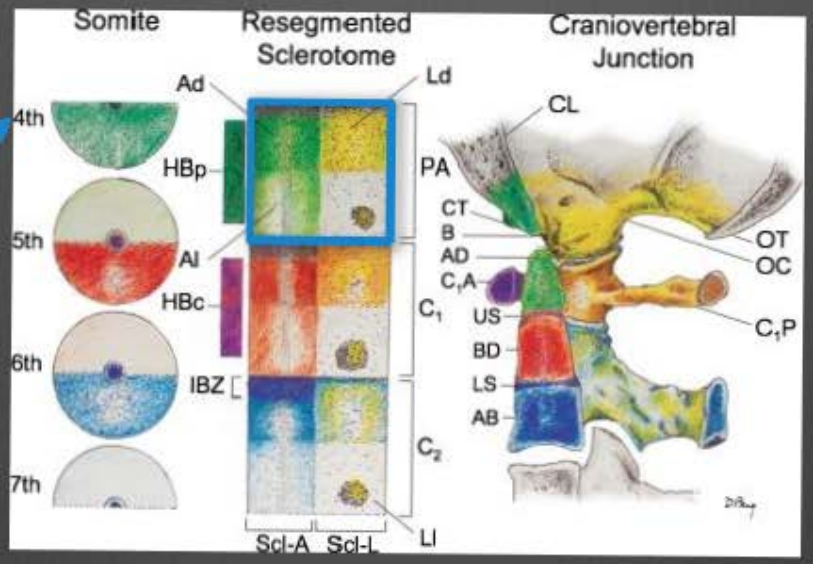
Somite
Resegmented Sclerotome
Craniovertebral Junction
4th
5th
6th
7th
Ad
HBp
AI
HBc
IBZ
Ld
PA
C1
C2
LI
Scl-A
Scl-L
CL
CT
B
AD
C1A
US
BD
LS
AB
OT
OC
C1P

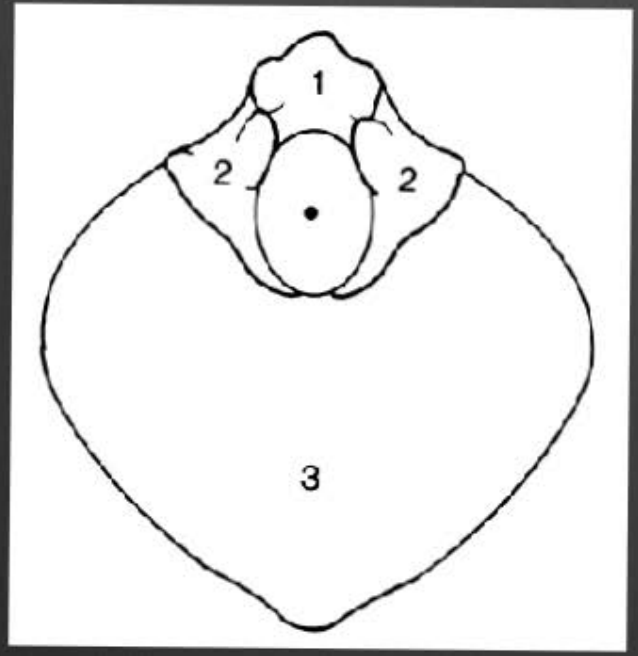
1
2
2
3

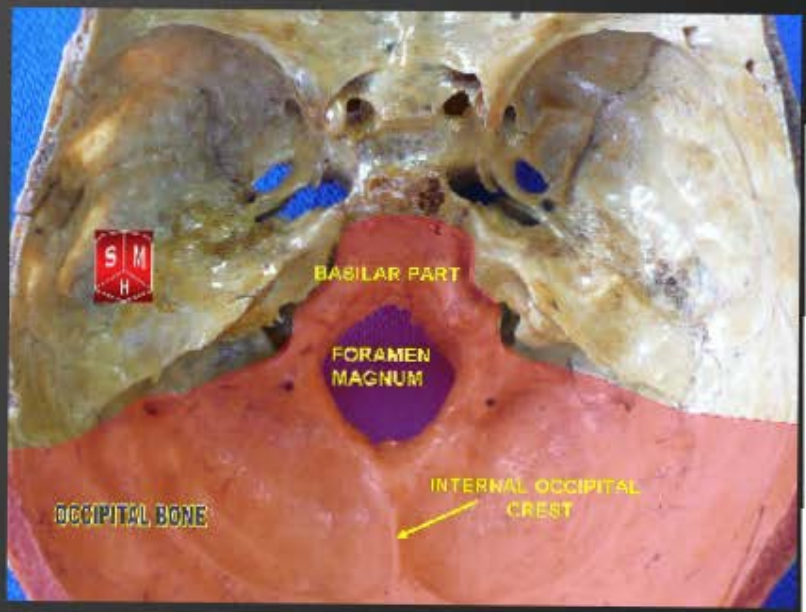
BASILAR PART
FORAMEN MAGNUM
INTERNAL OCCIPITAL CREST
OCCIPITAL BONE

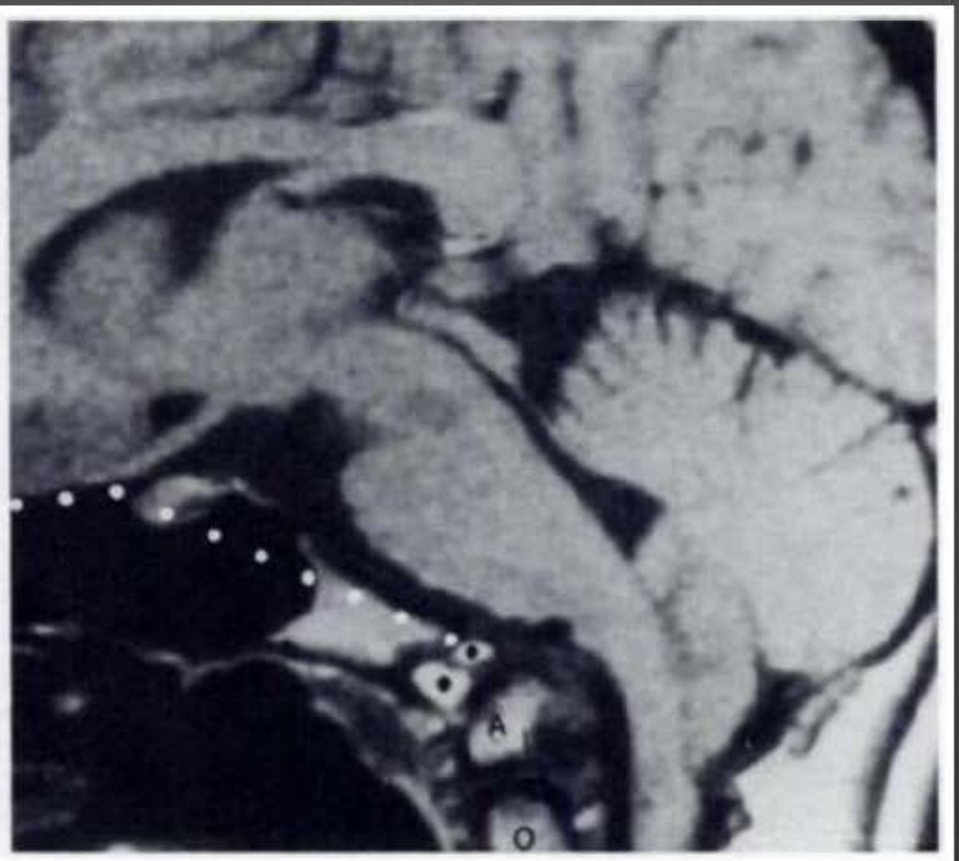

Figure 10. Condylus tertius and platybasia. Midsagittal T1-weighted (600/20) MR image reveals marked skull base flattening, with a Welcher basal angle of 150° (dotted line). Note the marked bowstring deformity of the cervicomedullary junction. The C-1 arch (*A*) lies directly above the tip of the odontoid process (*O*). Marrow within accessory ossification centers (condylus tertius) (black dots) is seen at the tip of the basion.

Supraoccipit

- Not purely derived from sclerotomes
- Endochondral and Membranous ossification

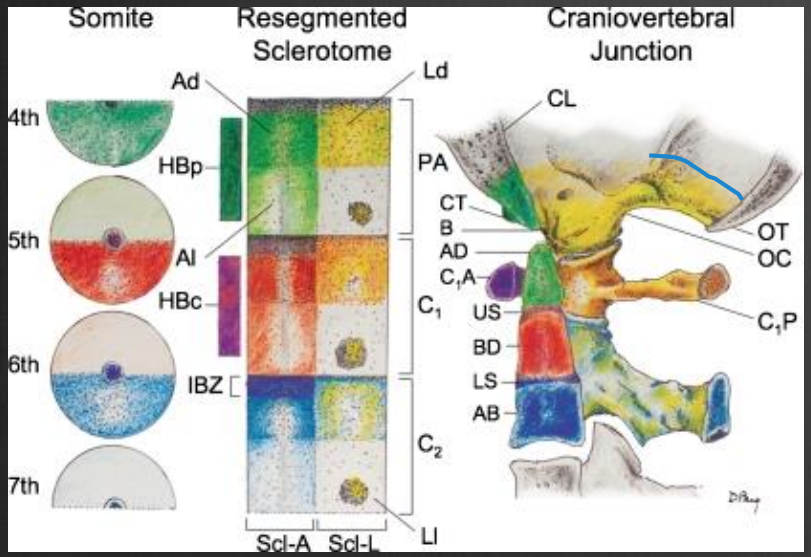

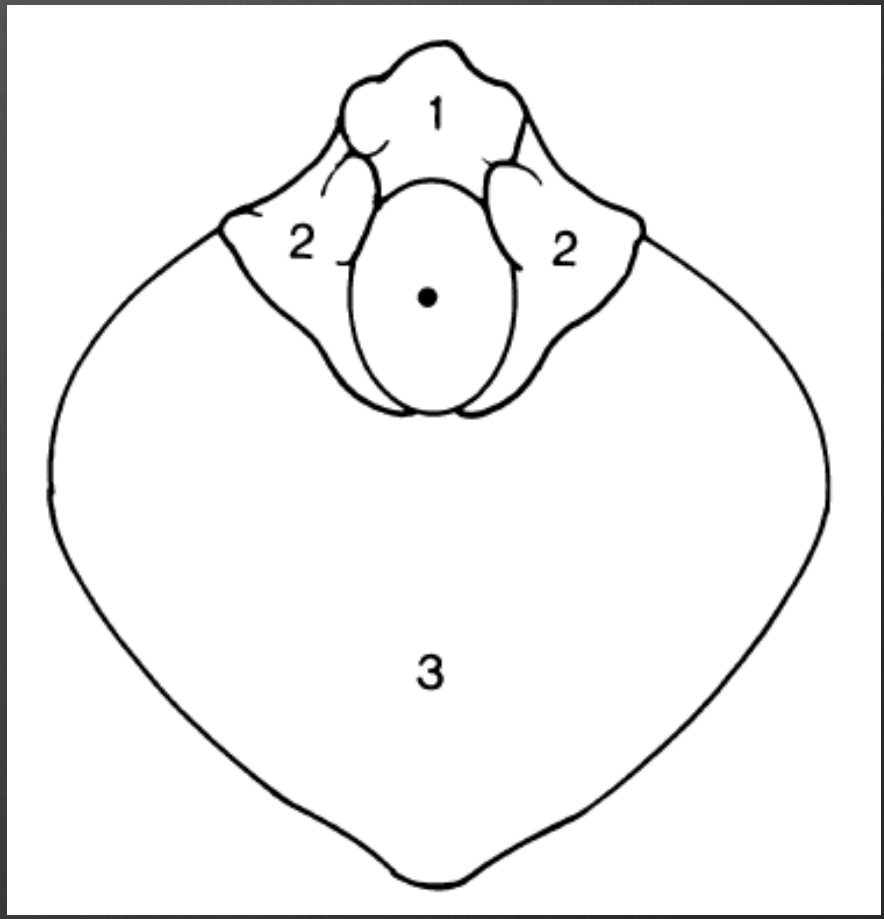

Differentiating a Mendosal Suture from a Skull Fracture

A 6-day-old infant was brought to her pediatrician with a right clavicle fracture. This injury could have happened at birth; however, the history provided by her mother was concerning enough that a skeletal survey and additional tests were performed and child protective services was notified. The lateral skull film seemed to show an occipital skull fracture (Figure 1), and the results of computed tomography of the head showed a single defect in the bone window that seemed to correlate with the finding on plain film. Computed tomography of the head with 0.625-mm slices and 3-dimensional reconstruction (Figures 2 and 3) was performed on day of life 14. As shown by the arrows in Figures 2 and 3,

Figure 1. Lateral skull film. Arrows show what seems to be an occipital skull fracture.

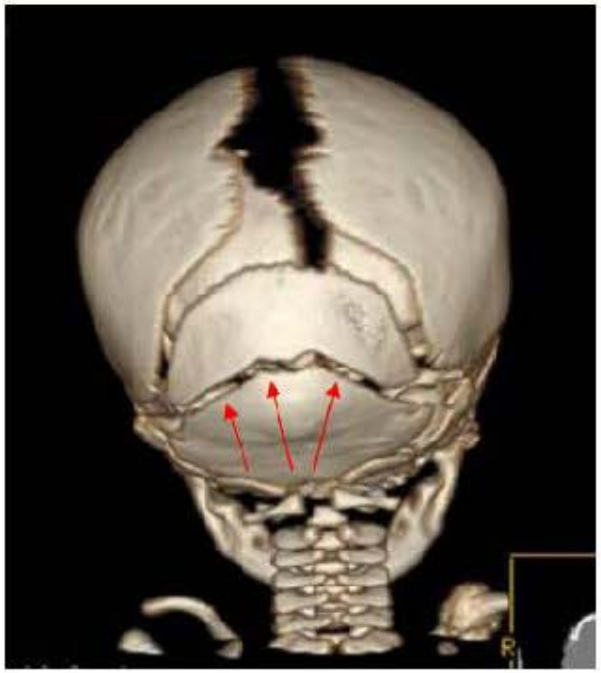

Figure 3. Three-dimensional reconstruction of computed tomography of the head, 0.625-mm slices. Arrows show persistent mendosal suture.

this patient has a rare, but classic, persistent mendosal suture. In utero, the mendosal suture separates the supraoccipital bone from the interparietal bone, and this suture usually closes in utero or in the first few days of life.[1] Performing the 3-dimensional reconstruction was key to determining that the

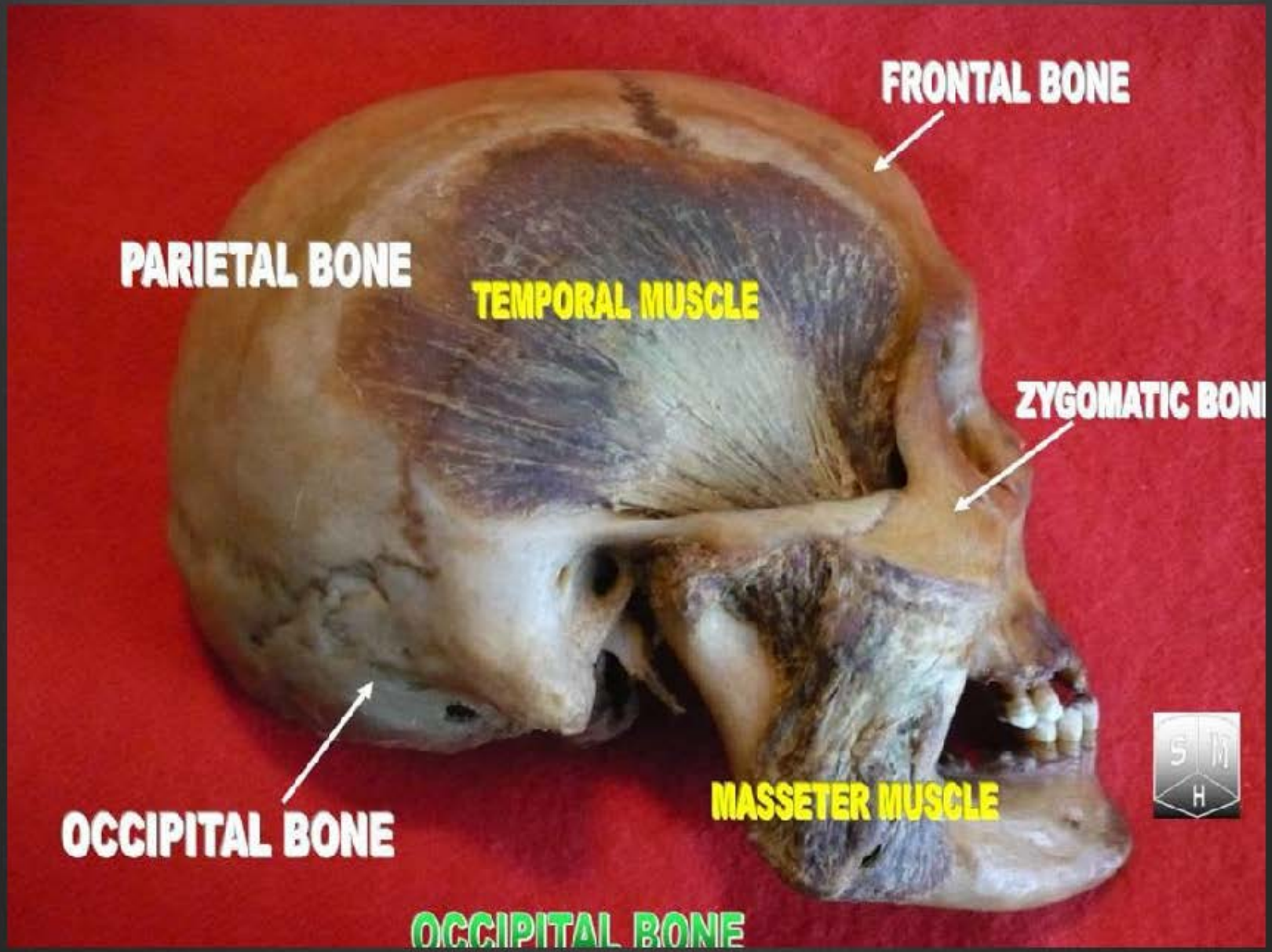
FRONTAL BONE
PARIETAL BONE
TEMPORAL MUSCLE
ZYGOMATIC BONE
MASSETER MUSCLE
OCCIPITAL BONE
OCCIPITAL BONE

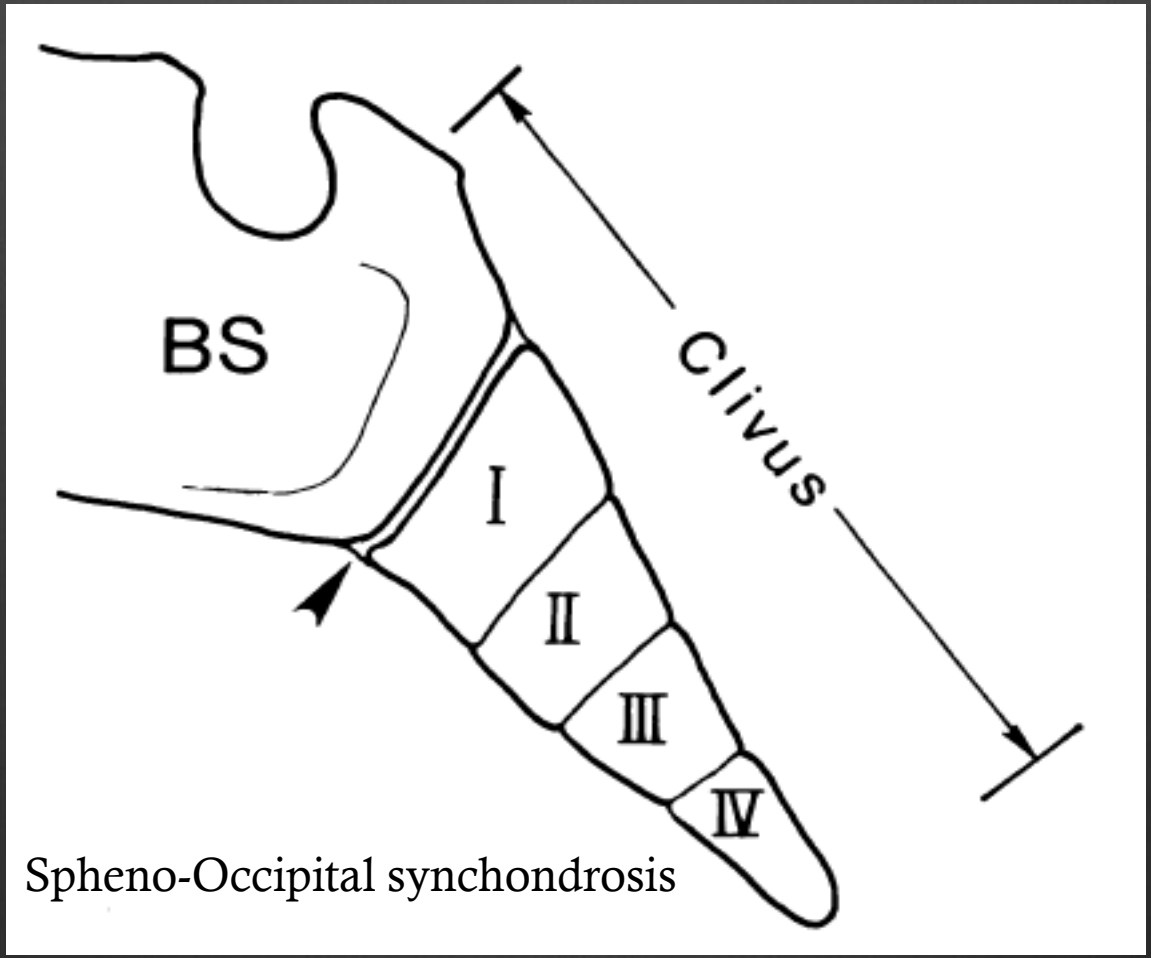

Spheno-Occipital synchondrosis

Roentgen Determination of the Time of Closure of the Spheno-Occipital Synchondrosis[1]

GEORGE LEIGH IRWIN, M.D.[2]

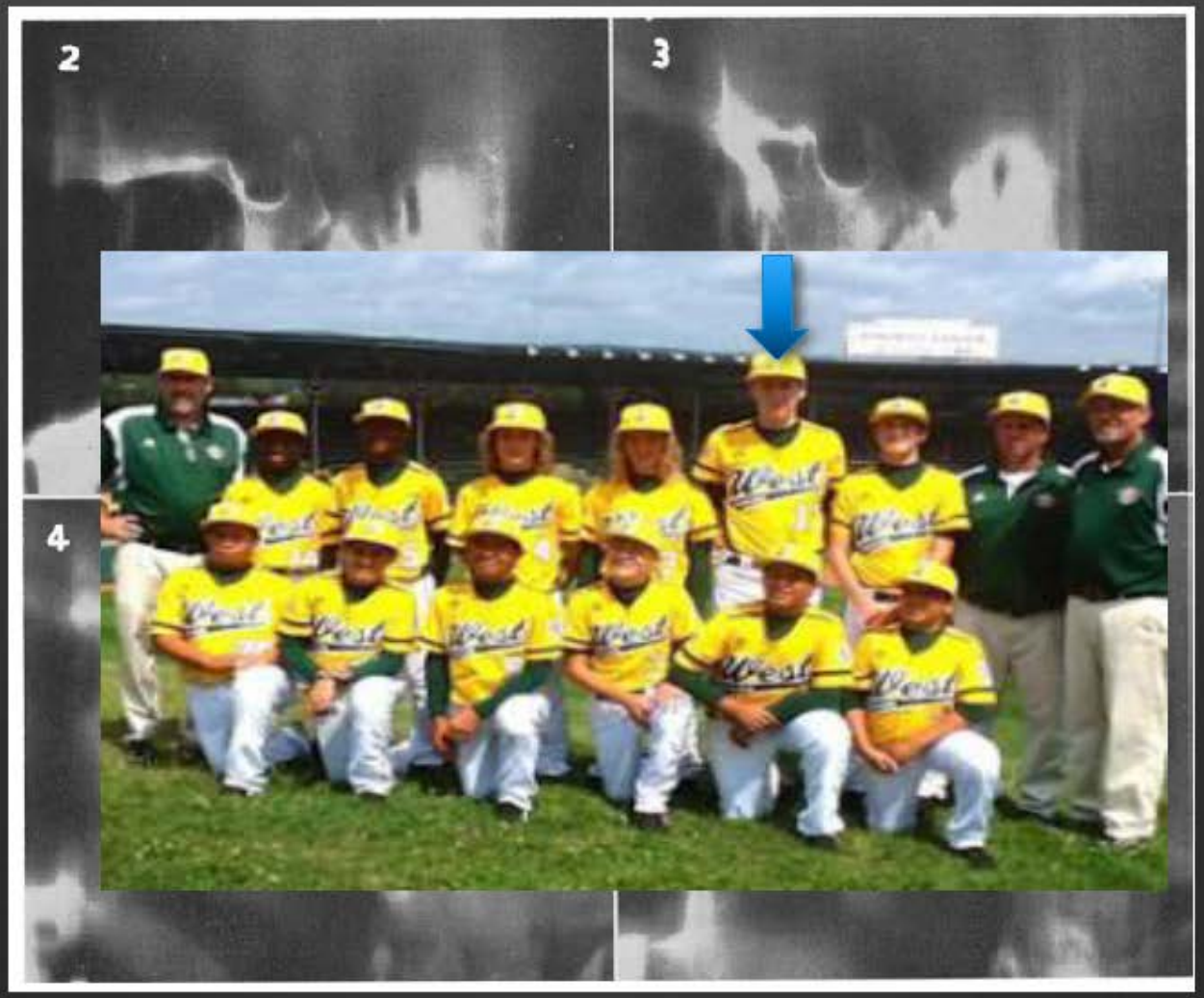

MR Imaging of the Normal and Abnormal Clivus

and the upper cervical spine, visualized on the cranial midline T1-weighted sagittal images, also showed diffuse loss of yellow marrow in these patients.

On T2-weighted images, lesions appeared as an area of homogeneously high intensity in three patients with chordoma, two with pituitary adenoma and one with nasopharyngeal carcinoma (Fig. 12). In five of eight patients with metastasis to the clivus, lesions were hyperintense relative to the normal clivus. The signal intensity was mixed with areas of iso- and hyperintensity in two patients with lymphomatous infiltration of the clivus (Fig. 10). The signal intensity was isointense relative to the normal clivus in three patients with metastasis, one with periclival meningioma and two with marrow reconversion. The diminished signal-to-noise ratio encountered on longer TR/TE images resulted in poorer anatomic definition of lesions.

Twelve of 21 patients with an abnormal clivus had gadopentetate-dimeglumine–enhanced scans. The low-intensity tumor, focal or diffuse, was intensely enhanced in all patients (Figs. 8 and 9). The reconverted clivus was mildly enhanced in one patient and moderately enhanced in the other (Fig. 11).

Discussion

Okada et al. [11], in their study of a group of normal children and young adults, demonstrated that signal from clival marrow was age-related and successively changed from uniformly low to uniformly high signal intensity on T1-weighted images. By the age of 24 years, 95% of their patients had a clivus of uniformly high signal intensity. The rate of conversion was somewhat slower in our patients. The clivus was uniformly bright in only one third of our normal patients in the third decade. The proportion of uniformly bright clivus gradually increases with advancing age. The rate increased to 80% by the eighth decade and reached 100% in the ninth decade. Our results show that interindividual variations are large in the composition of clival marrow in an adult population and that the conversion of red to yellow marrow occurs in a predictable and orderly pattern.

The hallmark of MR signal intensity caused by diseased marrow is T1 prolongation. The major factors determining the T1 changes are increased cellularity associated with tumor replacement of normal marrow and increased water content owing to bone marrow edema [10].

A clivus with uniformly low signal intensity that is hypointense relative to the pons should be considered abnormal in an adult patient. Conversely, a clivus of uniformly bright signal intensity is highly unlikely to be abnormal. The uniformly low signal intensity is attributable to diffuse tumor invasion of the clivus or marrow reconversion. In the normal adult, hematopoietic needs are met by the amount of red marrow existing

normal clivi. When contrast material is used, normal and abnormal clivi generally show different patterns of enhancement.

AJNR 11:1015–1021, September/October 1990; *AJR* 155:1285–1291, December 1990

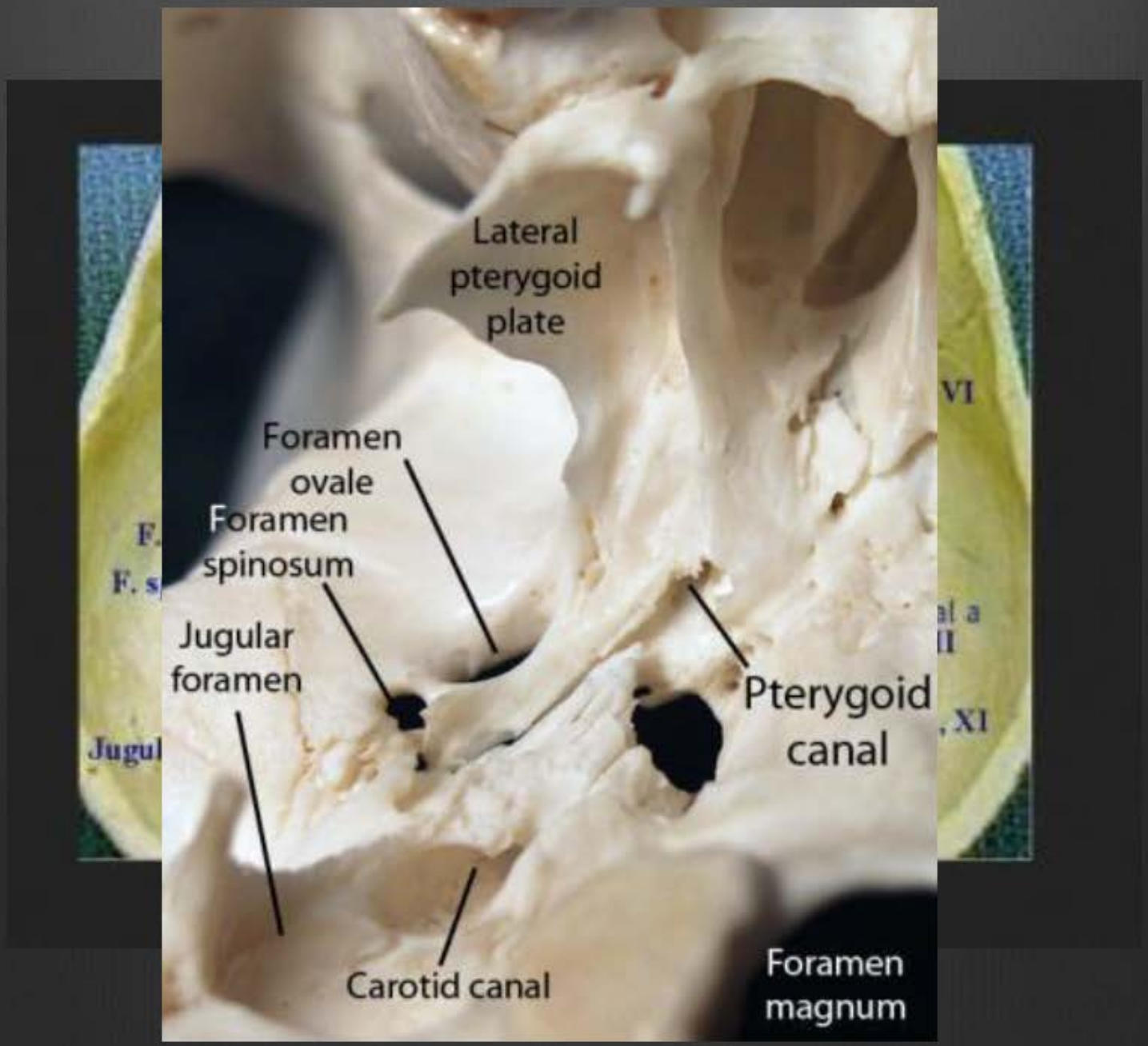
Lateral
pterygoid
plate
Foramen
ovale
Foramen
spinosum
Jugular
foramen
Pterygoid
canal
Carotid canal
Foramen
magnum

Jugular Foramen

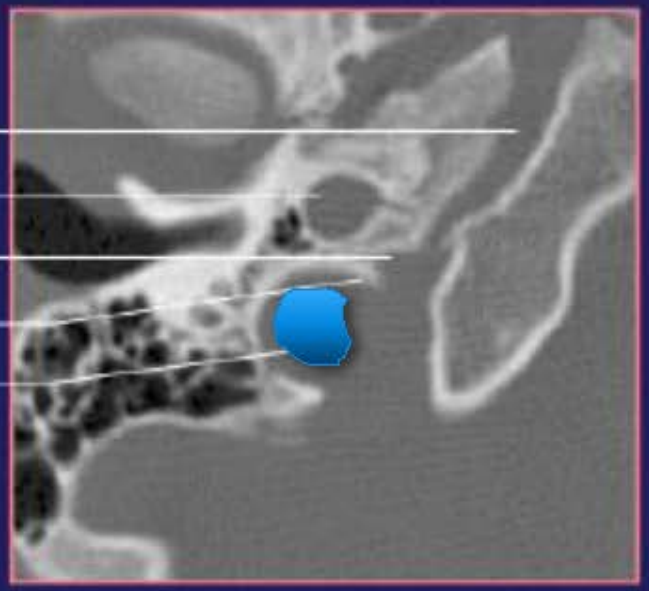

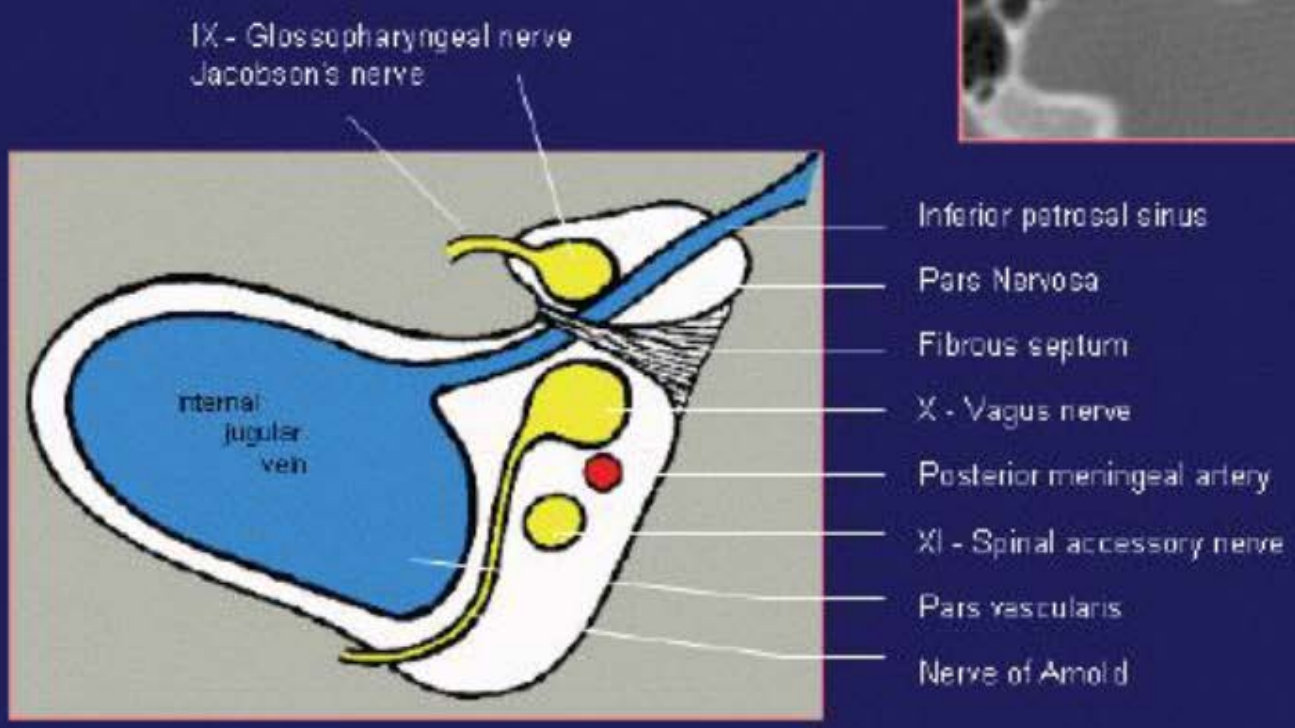

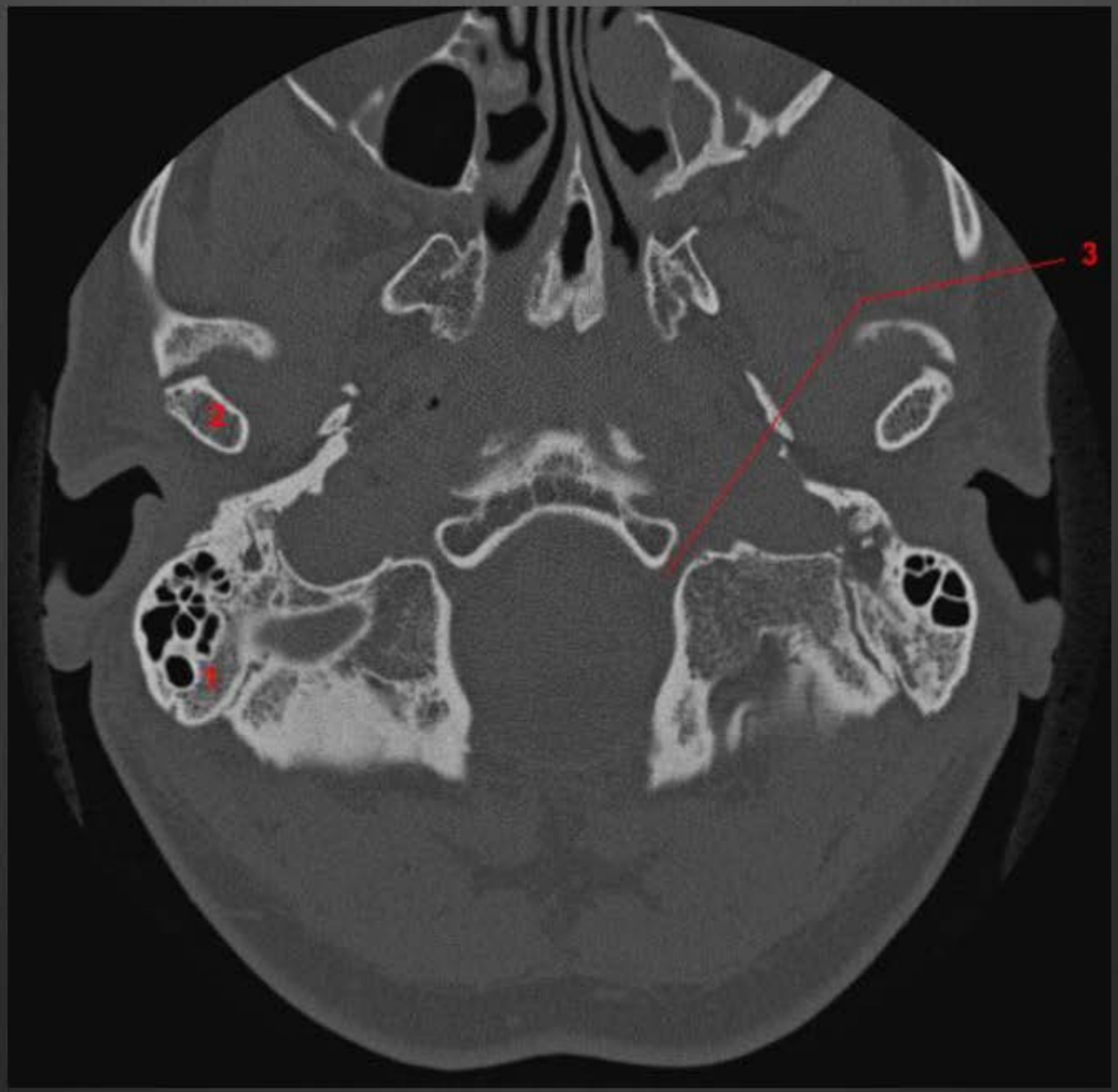
3
2
1

CASE 1

24-year-old woman with right side of tongue numbness, occasional hoarseness of her voice and difficulty swallowing.

IGNORE LEFT COCHLEAR IMPLANT

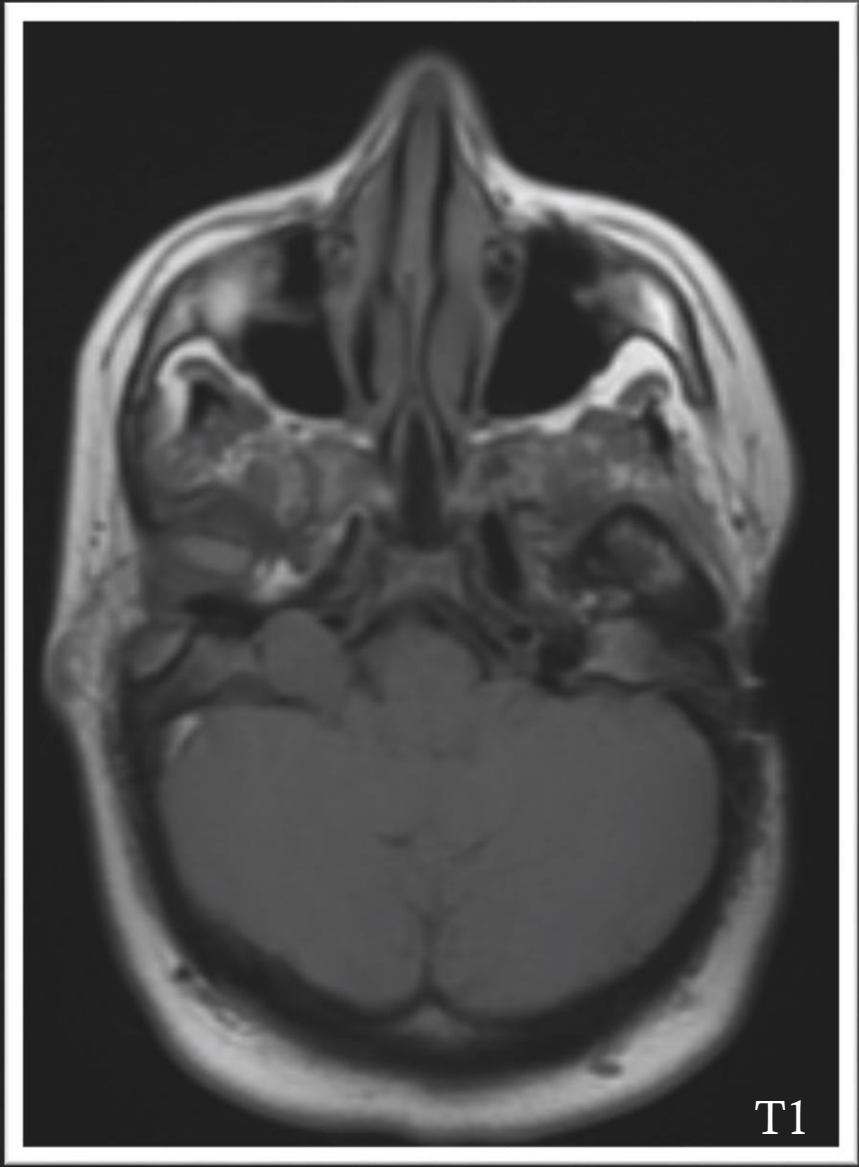
T1


T2

Lesions of the Jugular Foramen

- Glomus Tumor
- Schwannoma or Neurofibroma
- Meningioma
- Nasopharyngeal Carcinoma
- Metastatic Disease
- Slow Flow
- Enlarged or high riding bulb; diverticulum

Pathology

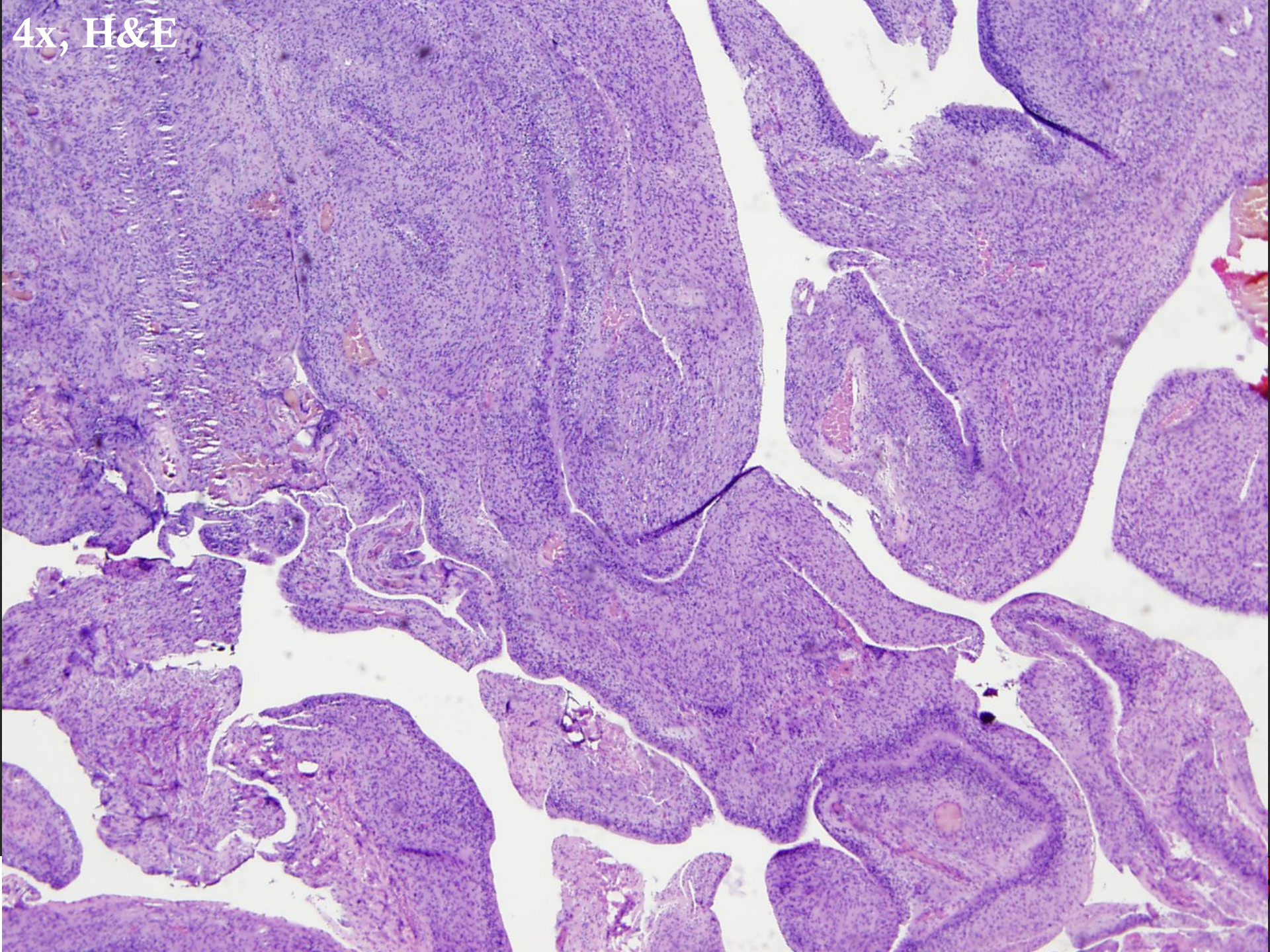
4x, H&E

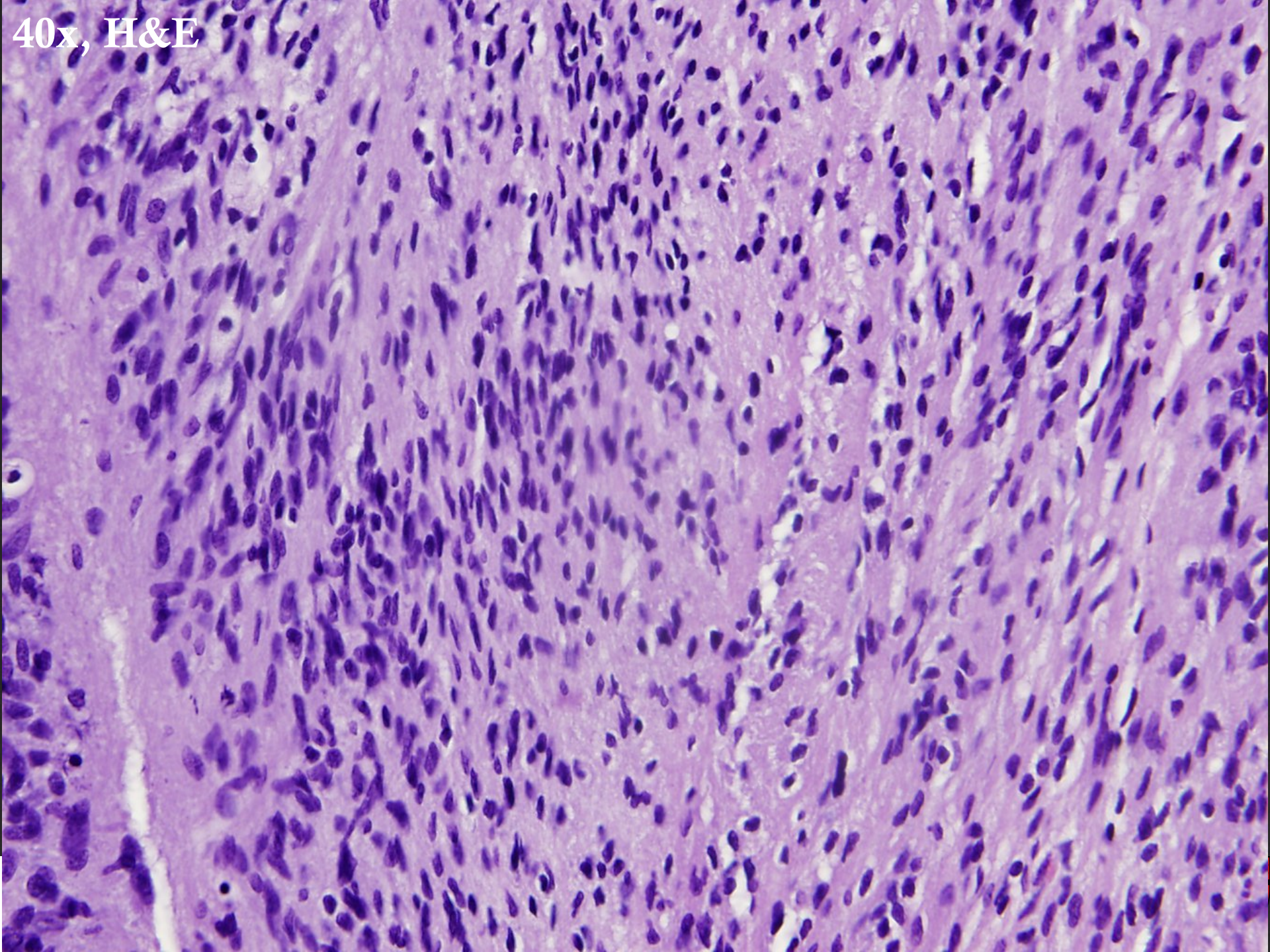
40x, H&E

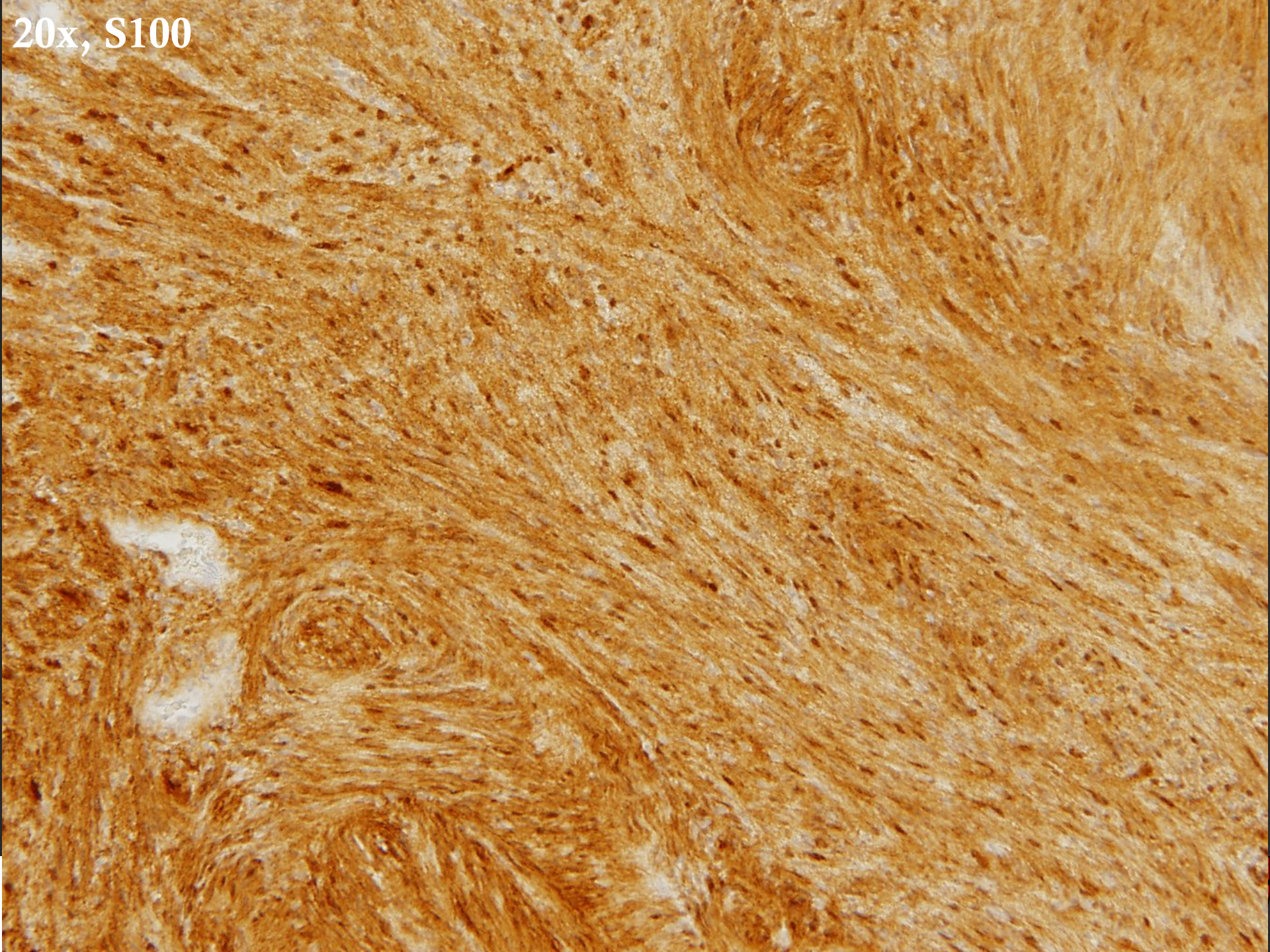
20x, S100

Final Pathologic Diagnosis

- **SCHWANNOMA**
  - Pos: S-100

Lesions of the Jugular Foramen

- Glomus Tumor
- Schwannoma or Neurofibroma
- Meningioma
- Nasopharyngeal Carcinoma
- Metastatic Disease
- Slow Flow
- Enlarged or high riding bulb; diverticulum

The Jugular Foramen: A Review of Anatomy, Masses, and Imaging Characteristics[1]

Karen S. Caldemeyer, MD
Vincent P. Mathews, MD
Biago Azzarelli, MD
Richard R. Smith, MD

Glomus Tumor vs. Schwannoma

	GLOMUS TUMOR	SCHWANNOMA
CT	Irregular Bone Erosion Hyperdense	Bone Expansion Sharp Borders Sclerotic Rim Isodense
T1 (rel. to WM)	'Salt and Pepper'	Hypo to Isointense
T2 (rel. to WM)	'Salt and Pepper'	Hyperintense Occasionally Cystic
Enhancement	+++ Early Drop Out	+
Behavior	Invade vein	Compress vein Dumbell shape

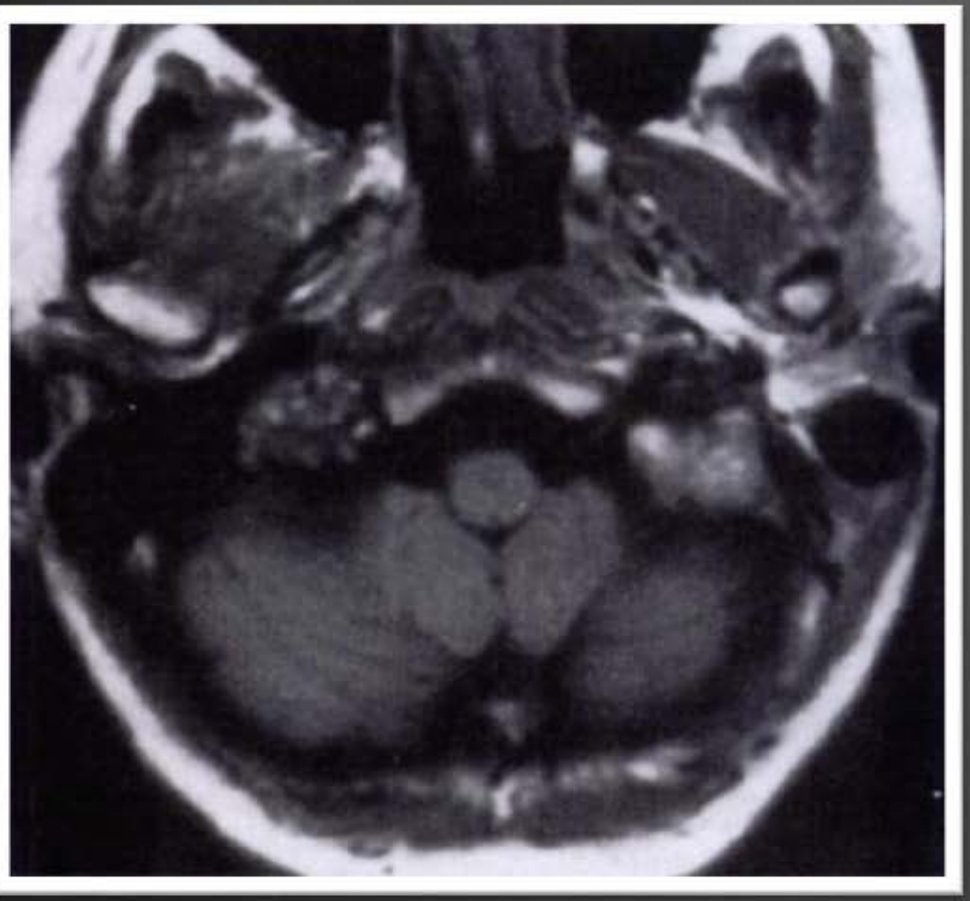

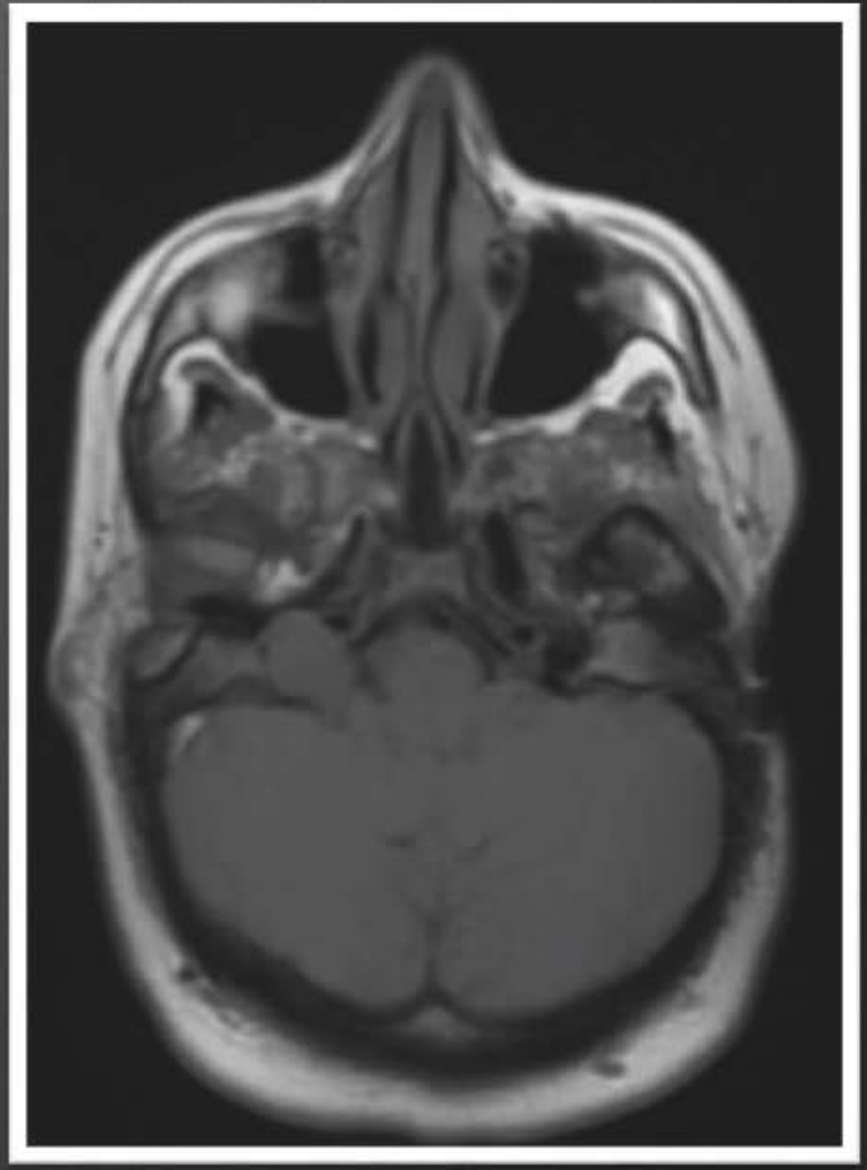

September-October 1997 Caldemeyer et al ▌ *RadioGraphics*

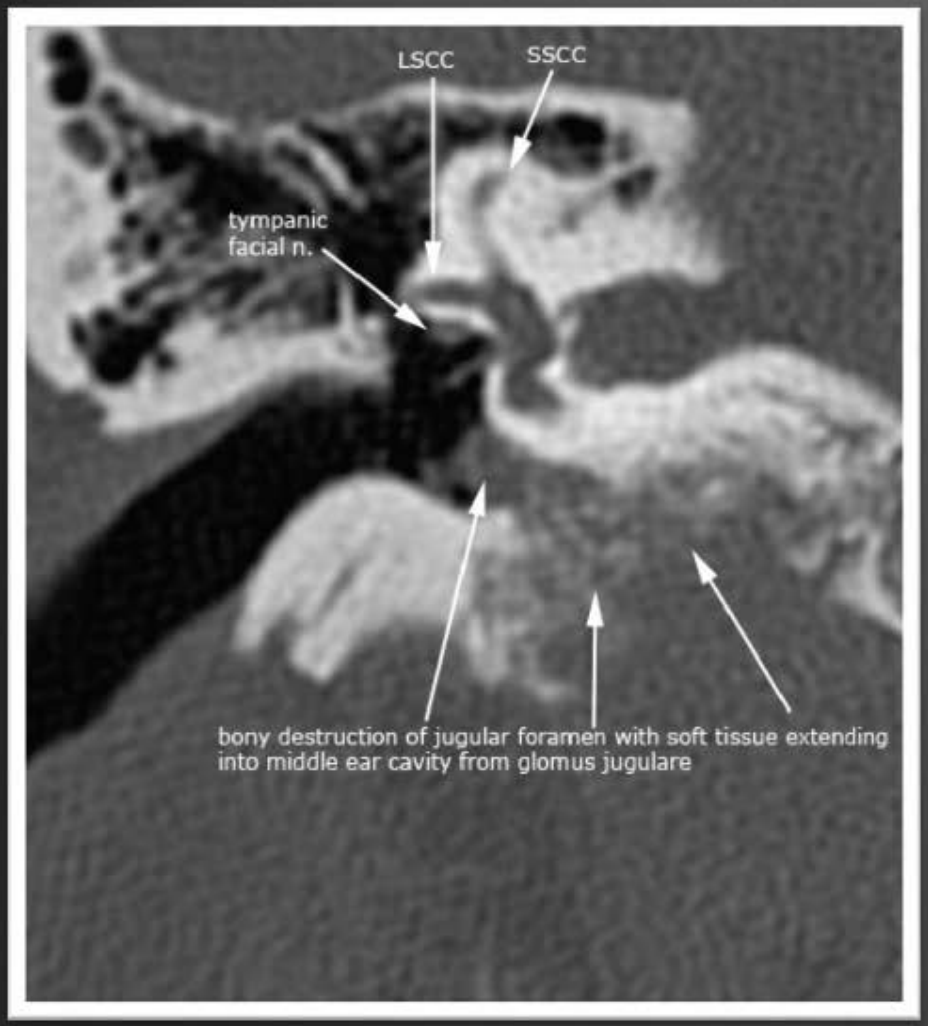
LSCC
SSCC
tympanic
facial n.
bony destruction of jugular foramen with soft tissue extending
into middle ear cavity from glomus jugulare

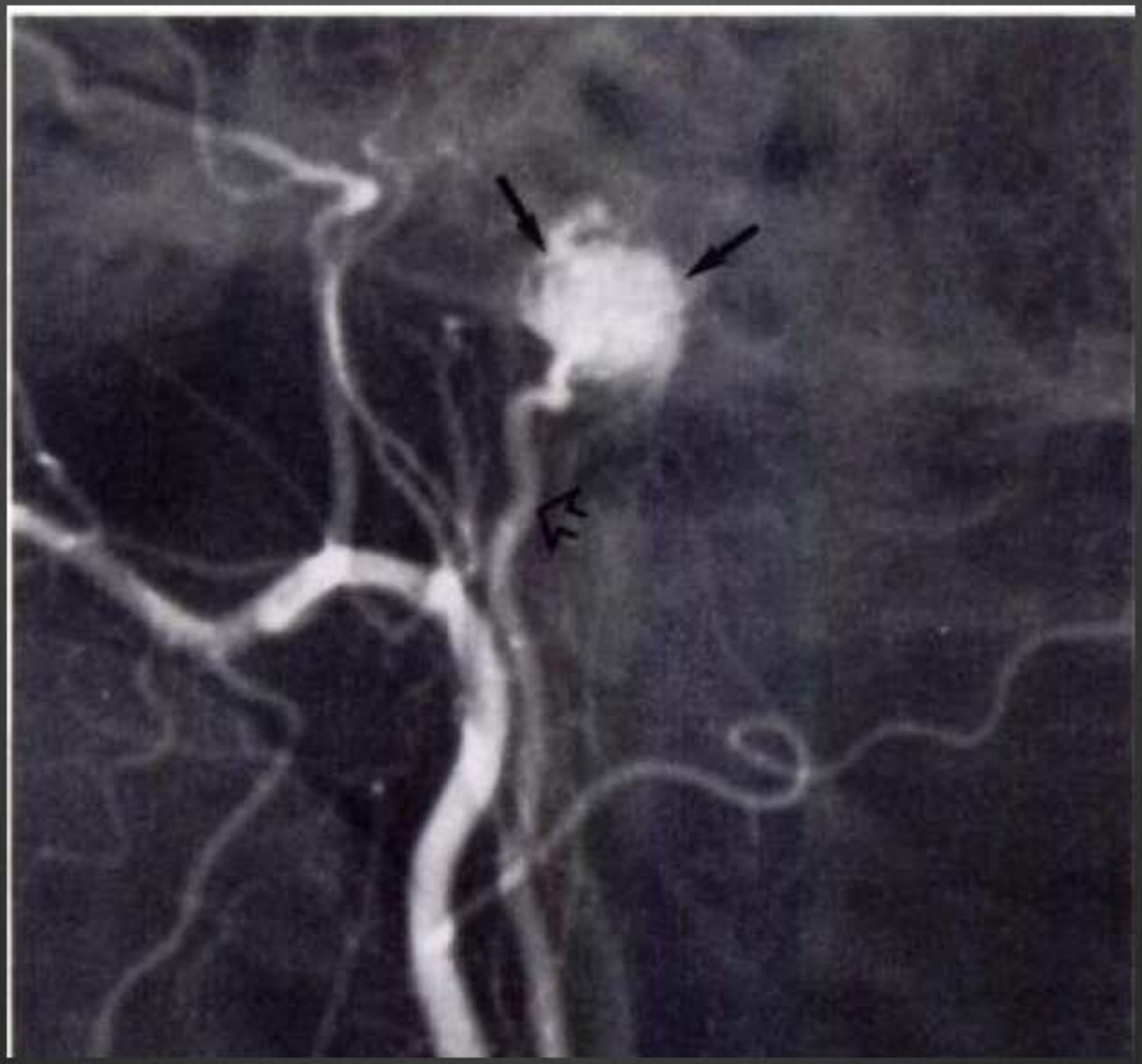

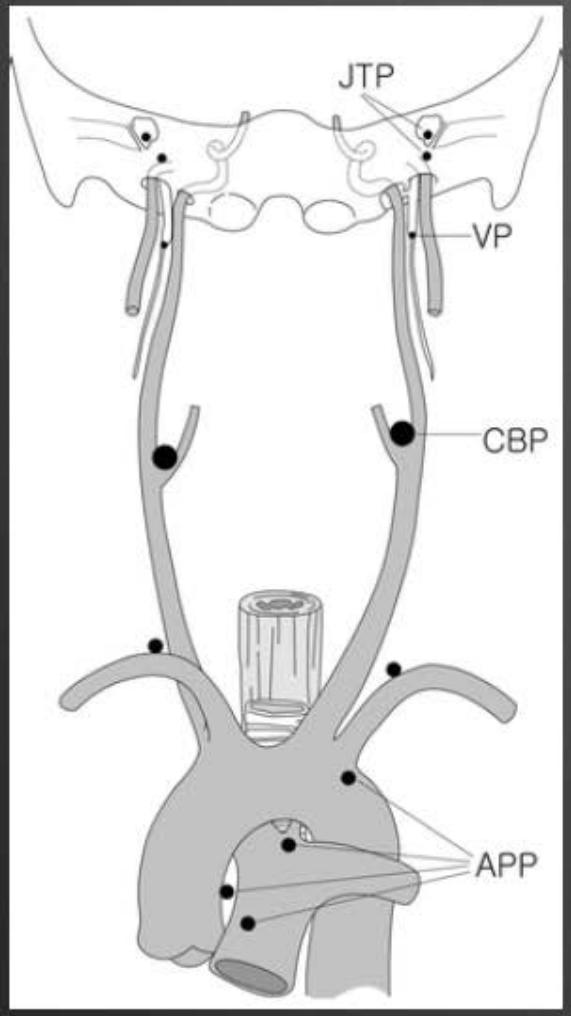

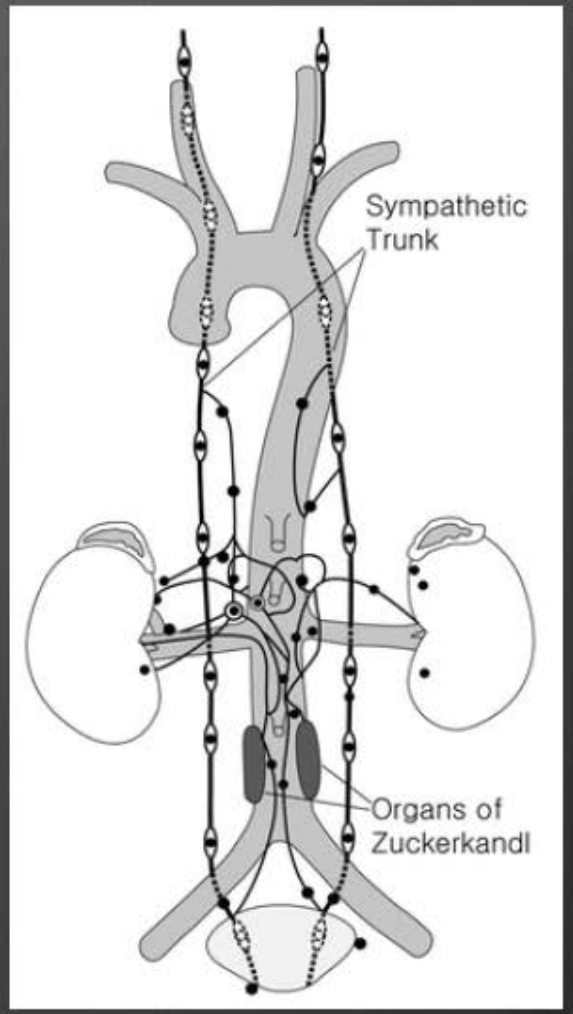

Lee et al.

AJR:187, August 2006

Case 2

22 year old male with diplopia and mild headache

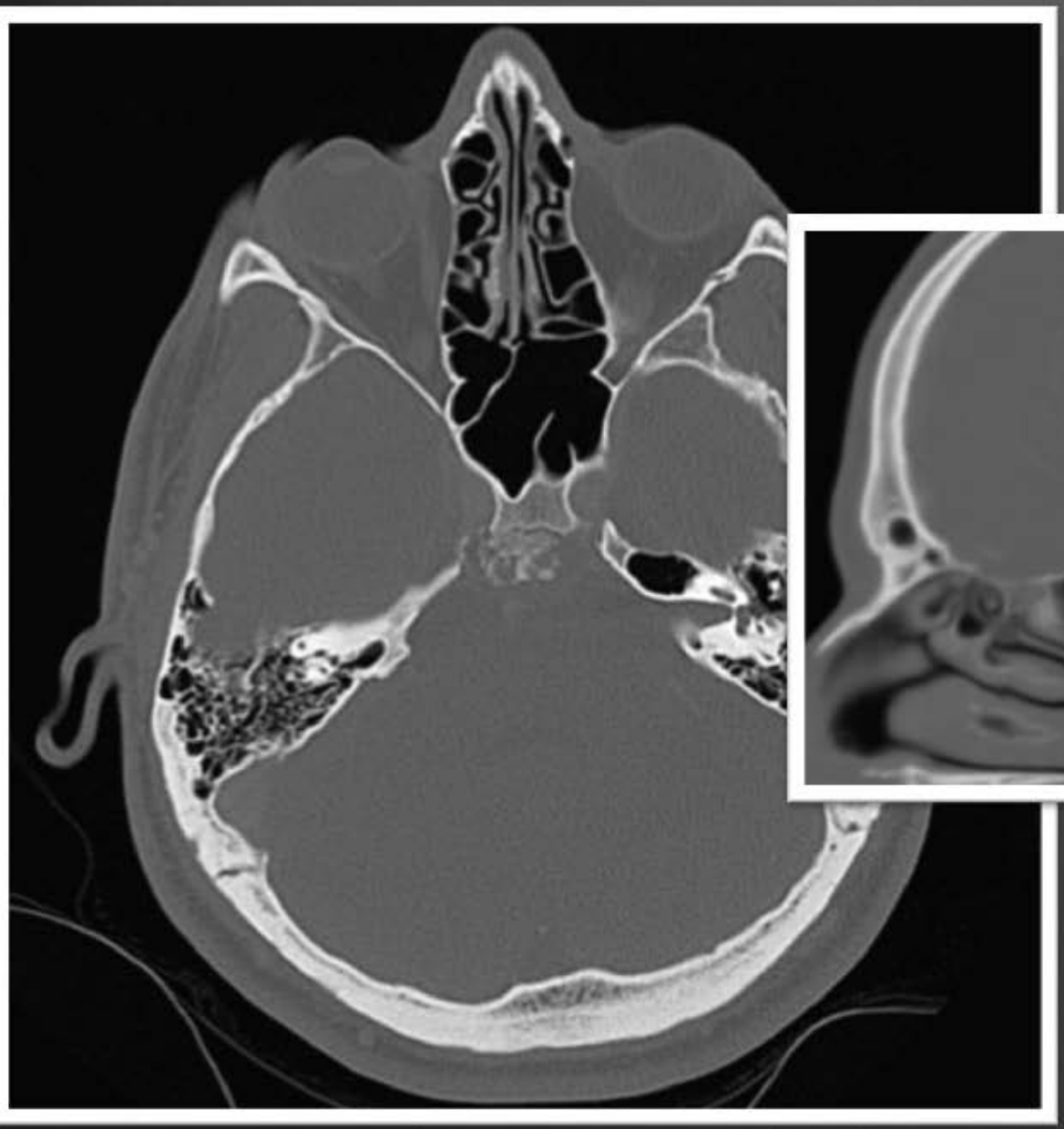

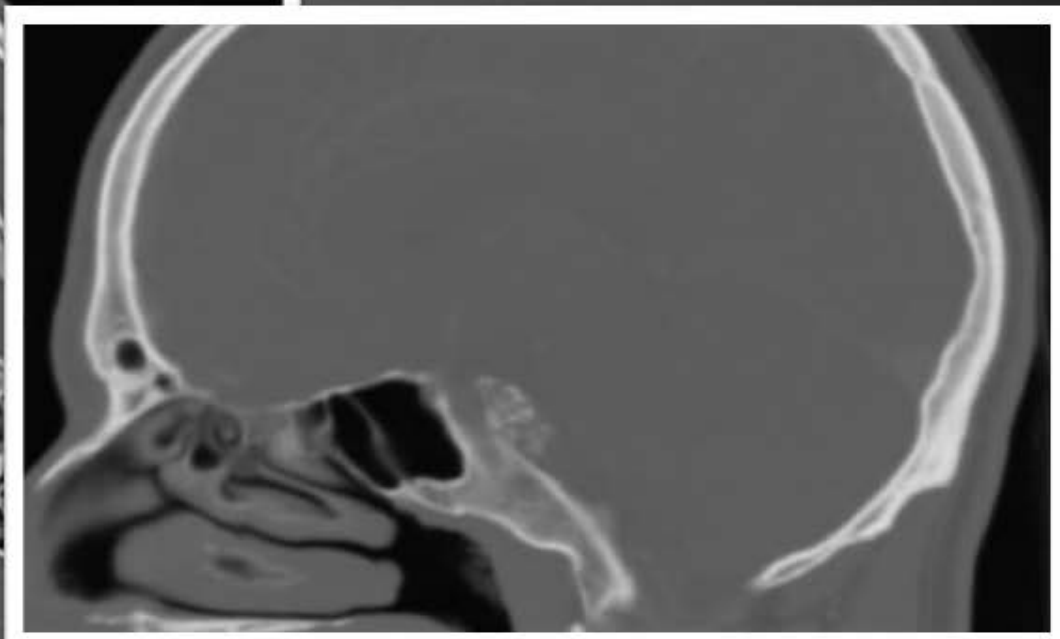

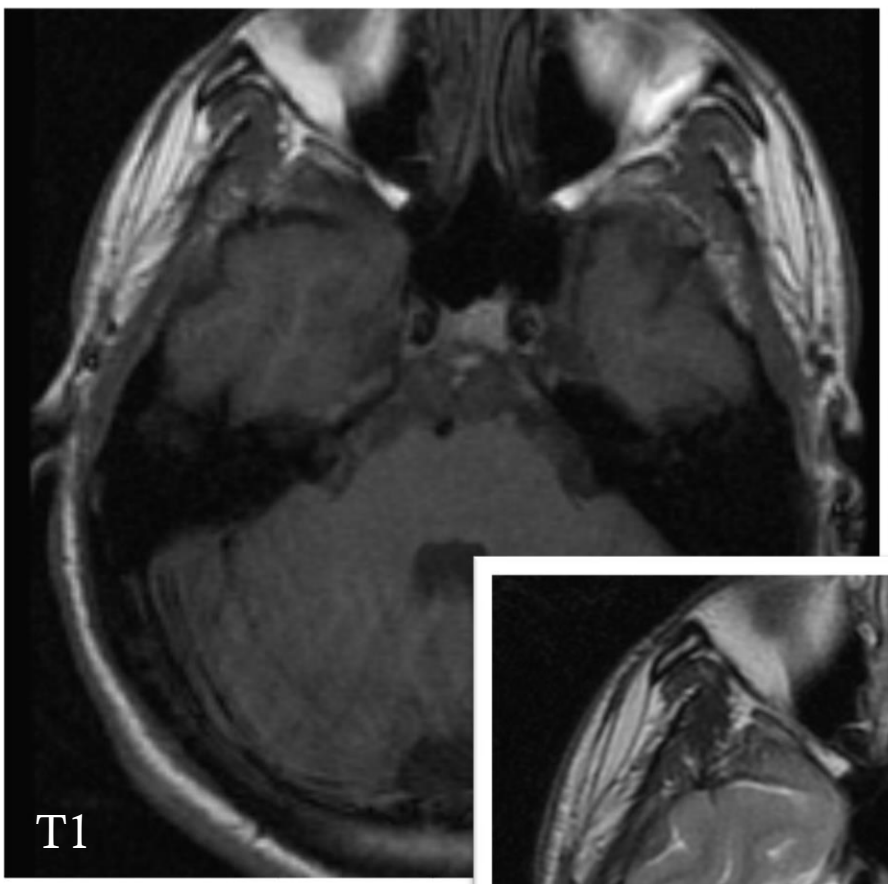
T1

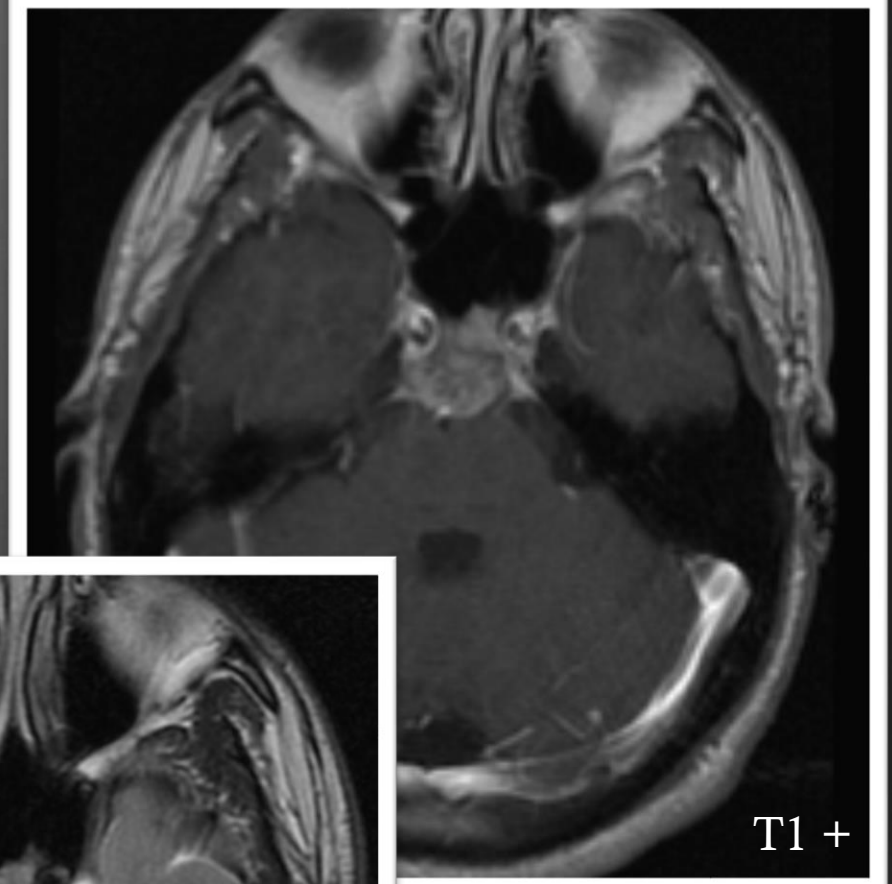
T1 +


T2

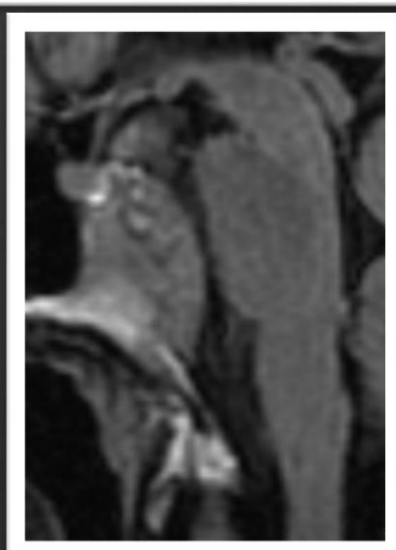

Lesions of Clivus

- Chondrosarcoma
- Chordoma
- Meningioma
- Plasmacytoma
- Metastasis
- Lymphoma
- Langerhans Histiocytosis
- Fibrous Dysplasia
- Infection

Pathology

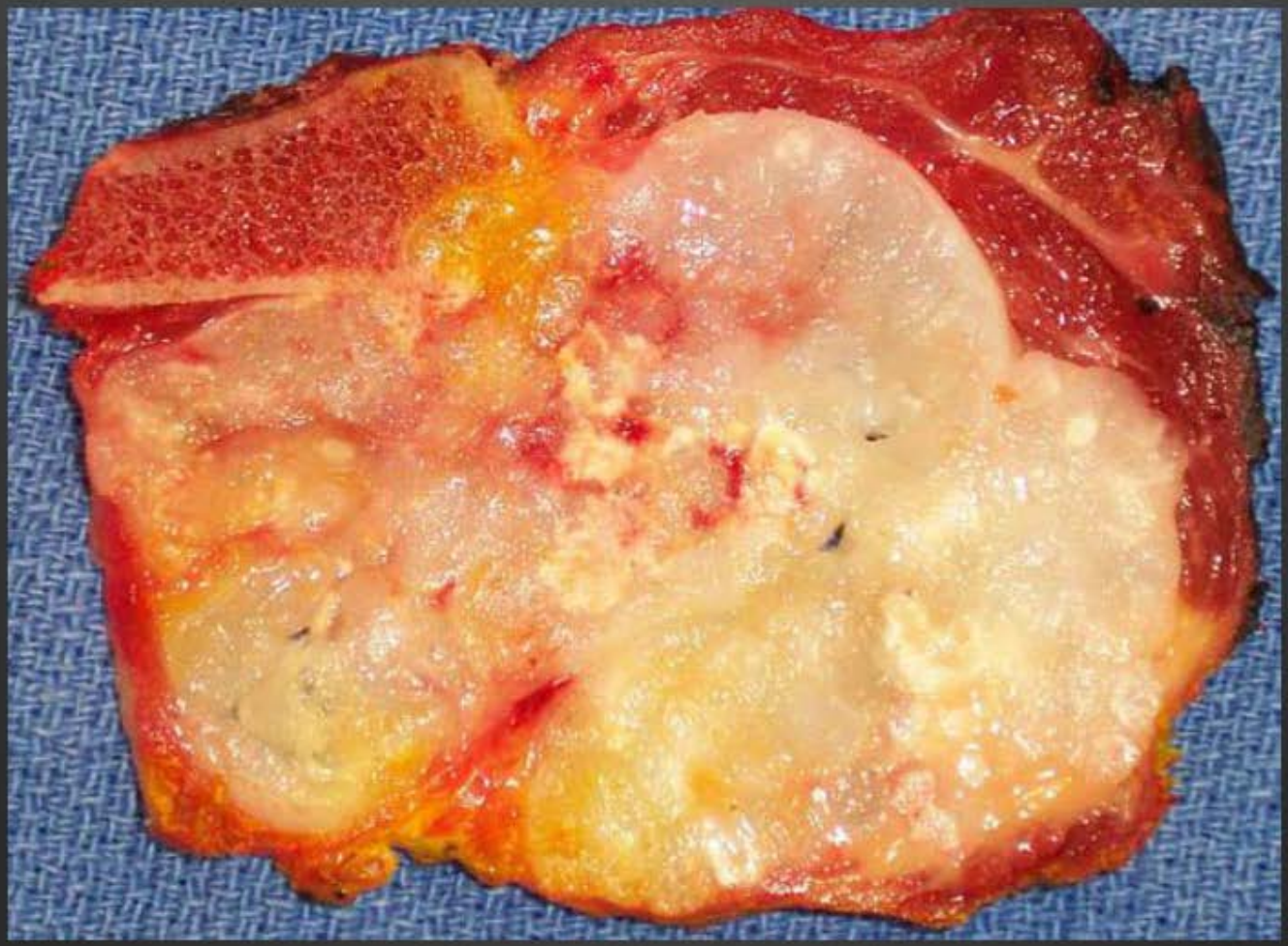

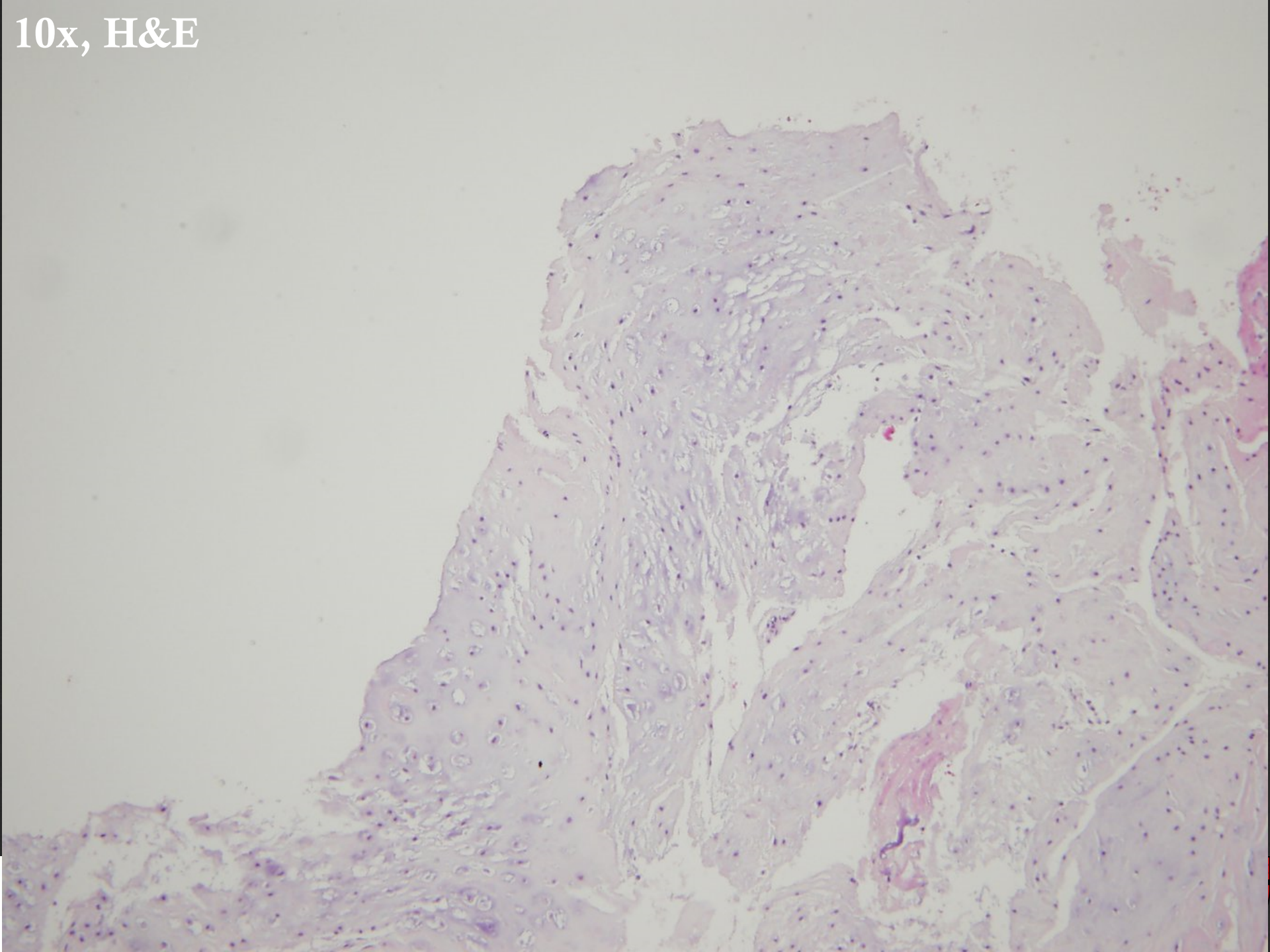
10x, H&E

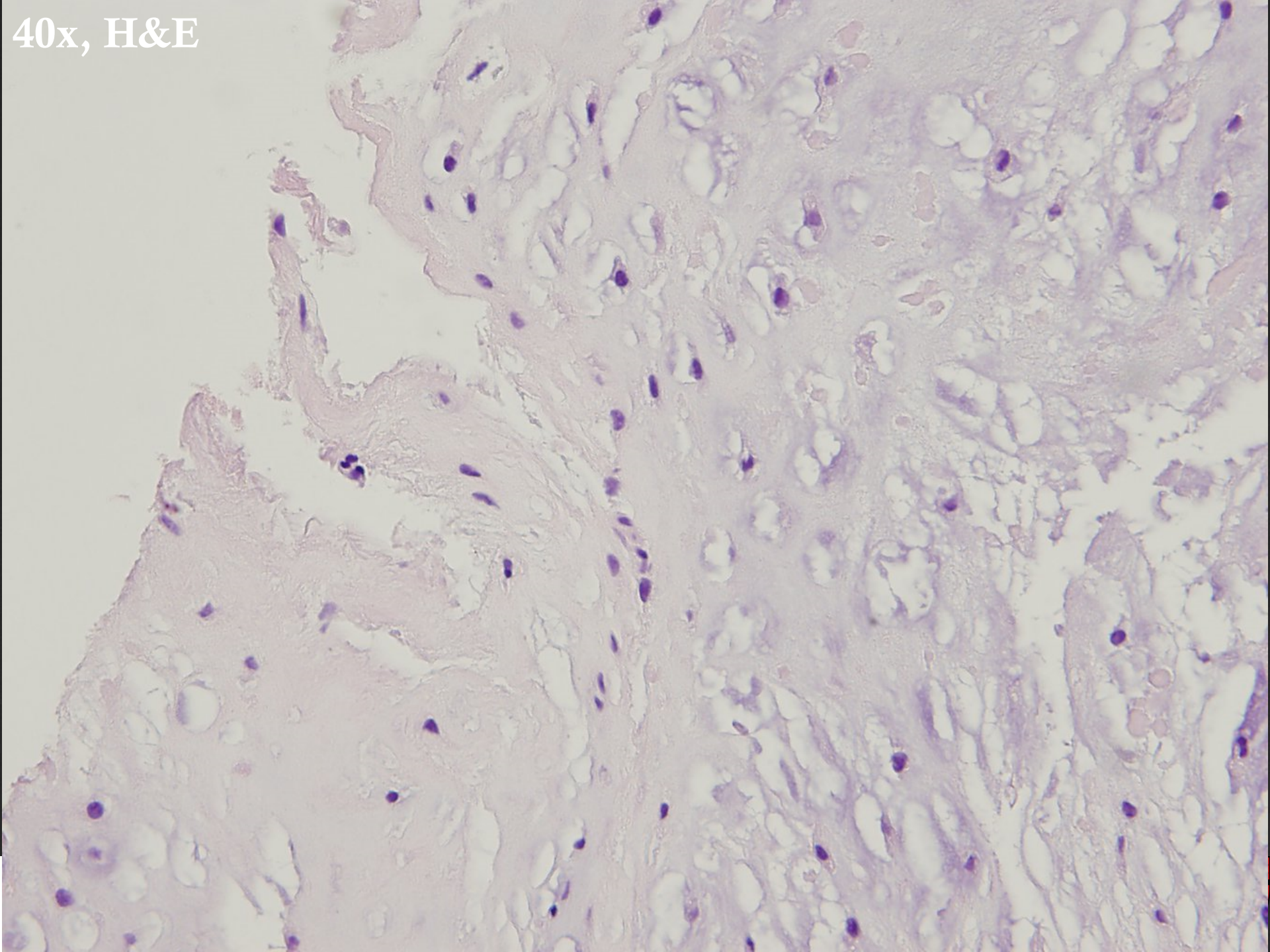
40x, H&E

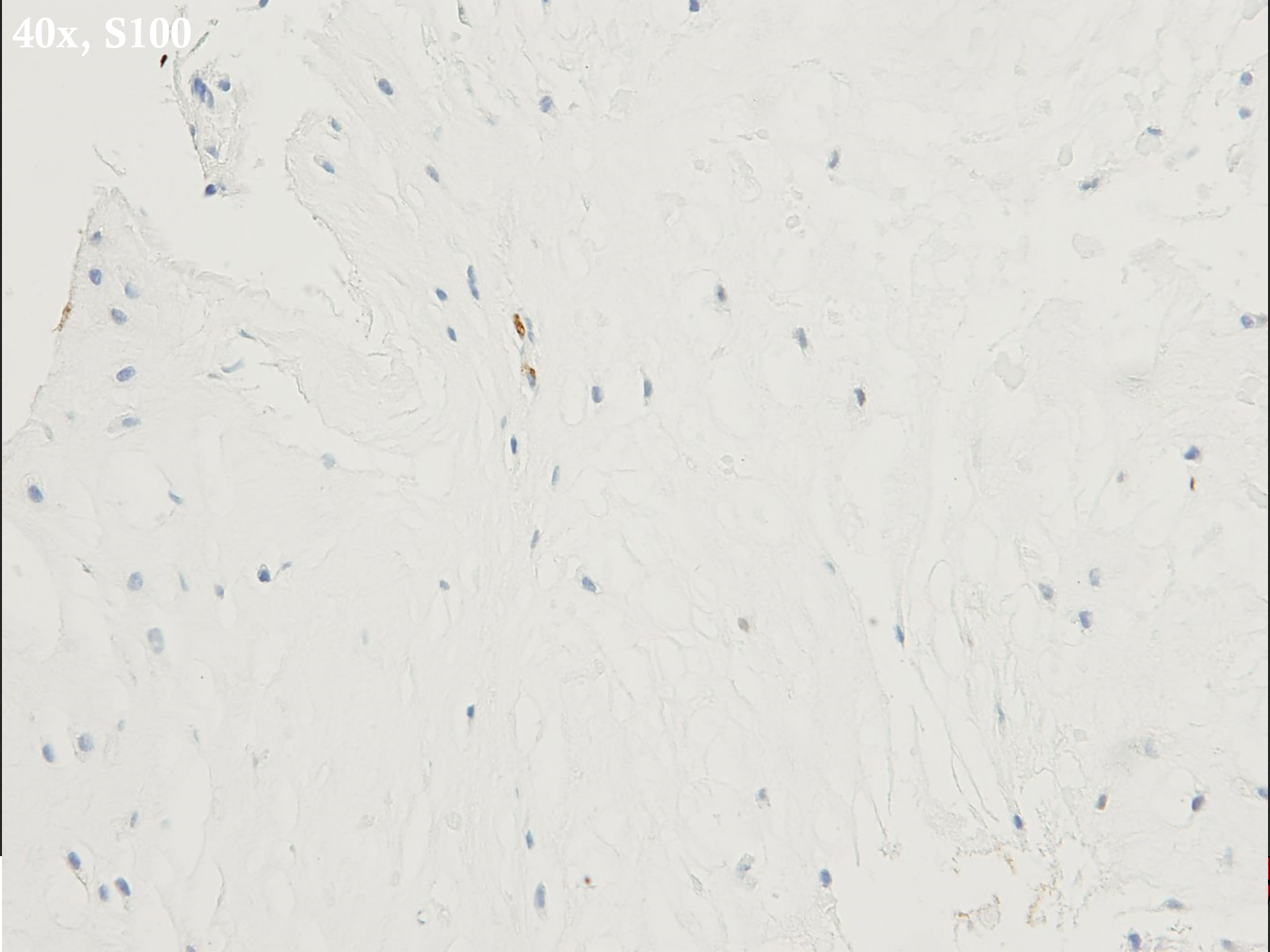
40x, S100

Final Pathologic Diagnosis

- **Well differentiated cartilaginous neoplasm, most c/w CHONDROSARCOMA**
  - Pos: S-100
  - Neg: EMA, Pan-K, CAM 5.2, AE1/AE3

Chondrosarcoma

- Mesenchymal origin malignant tumor with cells that produce cartilage matrix
  - Primary vs. Secondary
- Behavior is grade dependent

	Chondrosarcoma	Chordoma
CT	Rings and Arcs Linear Globular *Myxoid subtype	Well-circumscribed Variably Hyperattenuating Extensive lytic destruction *Chondriod subtype
T1 (rel. to WM)	Intermediate to Low	Intermediate to Low
T2 (rel. to WM)	Hyperintense	Hyperintense
Enhancement	+, heterogeneous	+, heterogeneous
Behavior	Less Common Majority arise from petro-occipital fissure Better prognosis	More common Midline typically Local Recurrence common Metastasis Rare

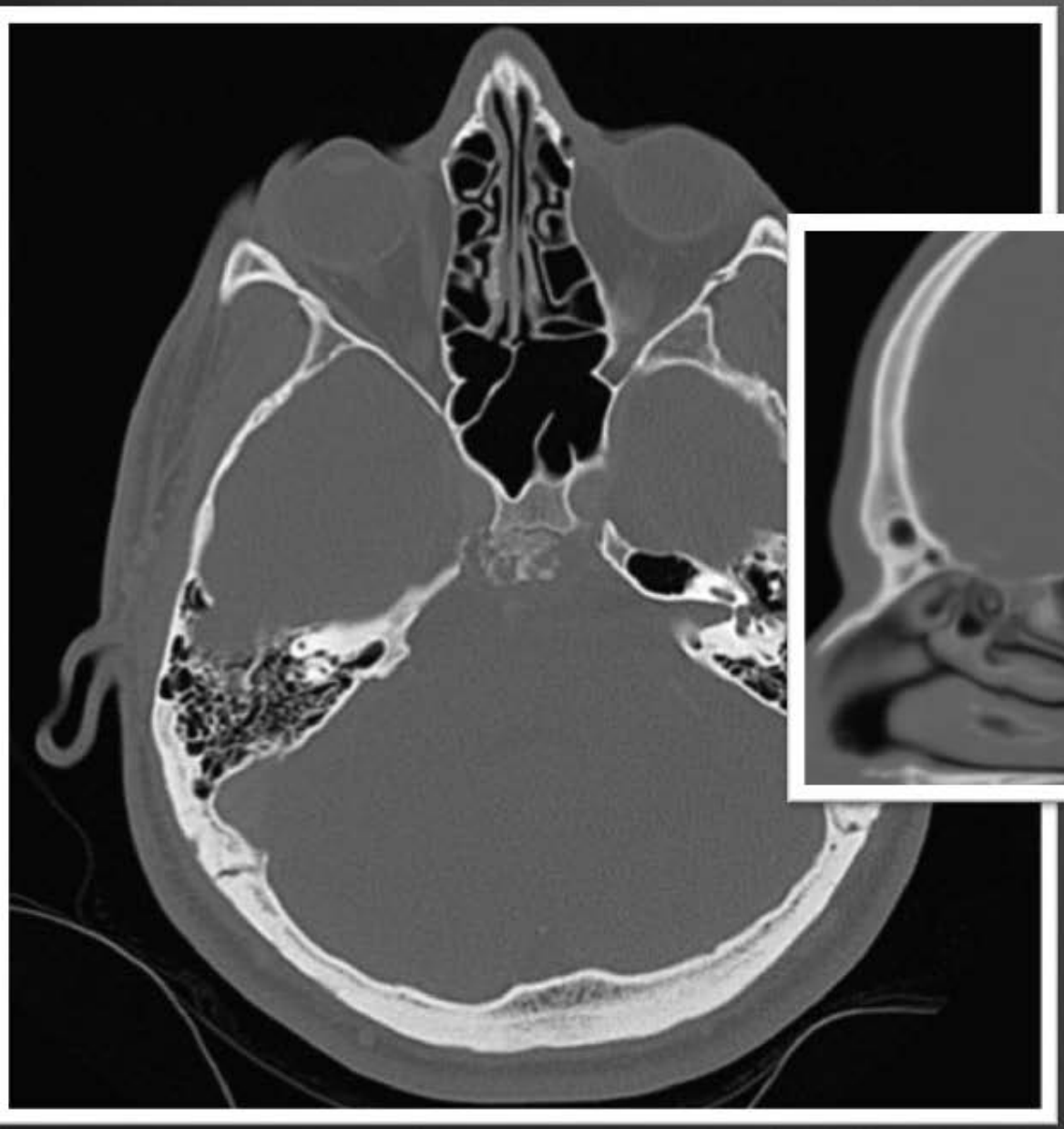

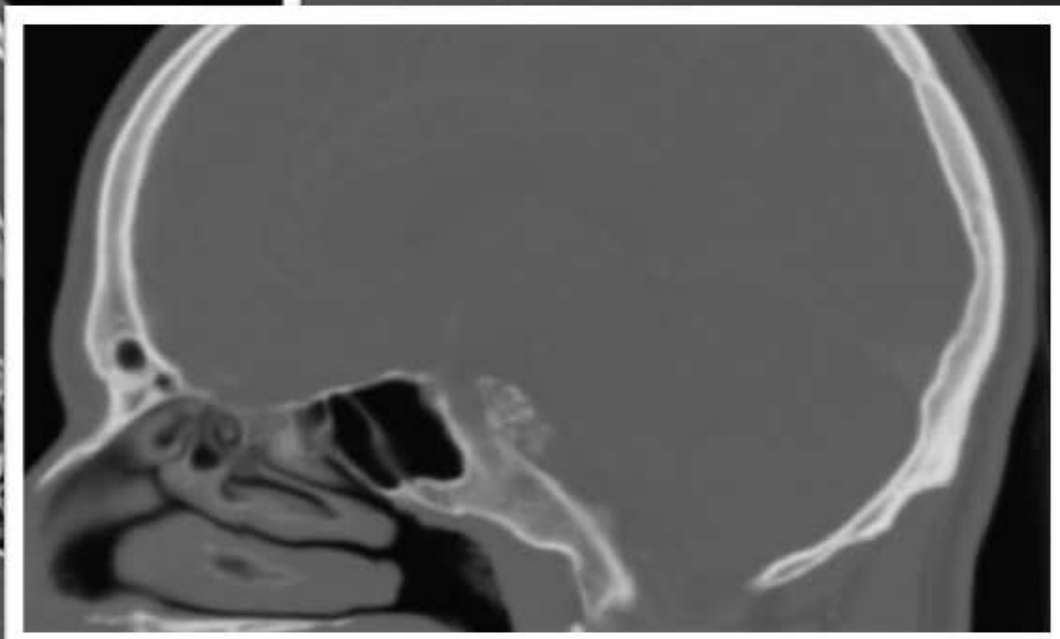

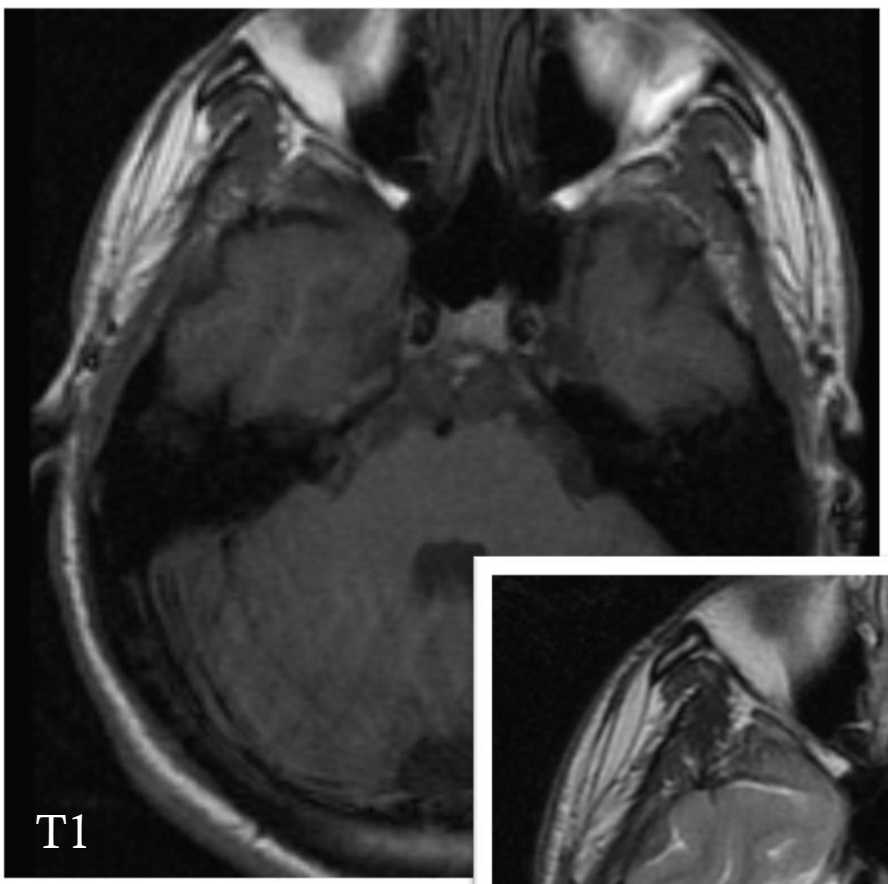
T1

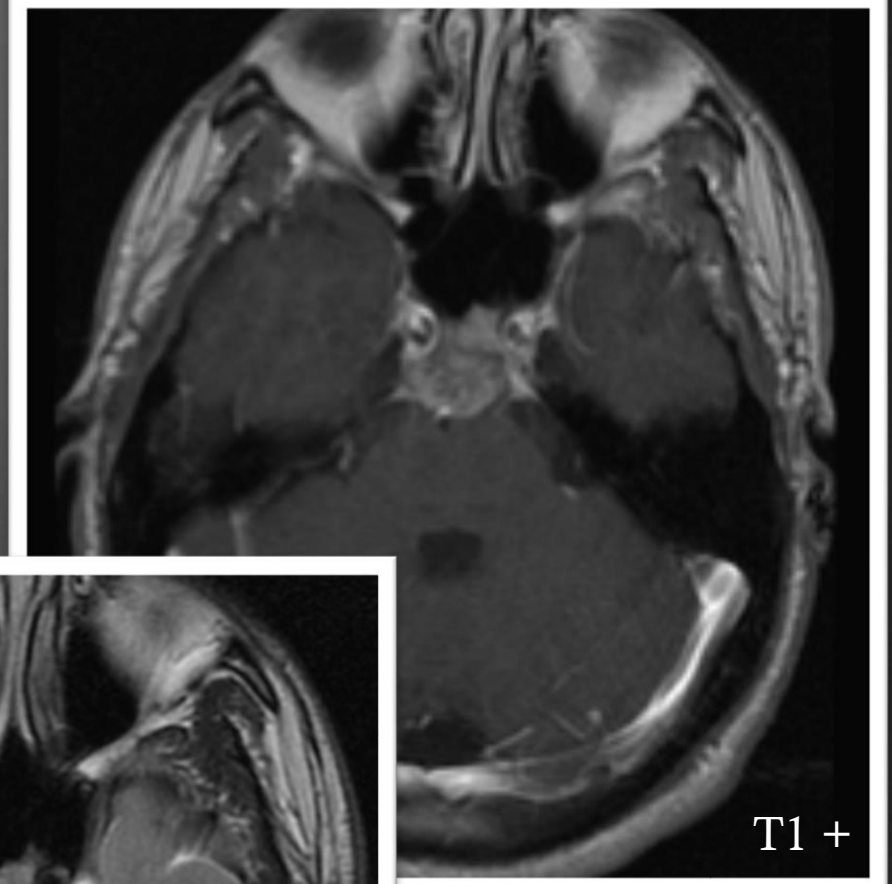
T1 +


T2

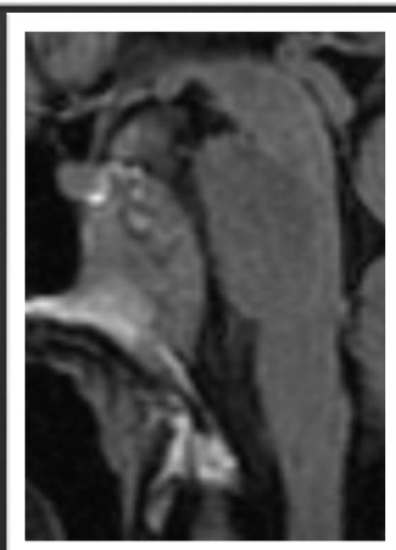

DWI: Hot of the Press

Diffusion-Wei…ase Chordoma

…ndrosarcoma

K.W. Yeom, …B. Edwards, and N.J. Fischbein

RESULTS: Chondrosarcoma was a…) and was significantly different from classic chordoma (1474 ± 11… 10^{-6} mm^2/s) ($P < .001$). Poorly differentiated chordoma was char… IR imaging features of enhancement and/or lesion location did n…

CONCLUSIONS: Diffusion-weigh… differentiating chordoma from chondrosarcoma. A prospective s… C in predicting histopathologic diagnosis.

Table 2: ADC values for each tumor type (10^{-6} mm^2/s)

Tumor	Mean ADC (Median)	Minimum ADC (Median)	Maximum ADC (Median)
Chondrosarcoma ($n = 9$)	2051 ± 262 (1977)	1488 ± 360 (1352)	2503 ± 512 (2392)
Classic Chordoma ($n = 7$)	1474 ± 117 (1460)	905 ± 118 (860)	2199 ± 255 (2217)
Poorly Differentiated Chordoma ($n = 3$)	875 ± 100 (871)	491 ± 210 (469)	1503 ± 127 (1557)

Table 3: MRI features for each tumor type

Tumor	T2 Hypointensity	>90% Enhancement	Clival Location
Chondrosarcoma ($n = 9$)	0 (0%)	5 (56%)	4 (44%)
Classic chordoma ($n = 7$)	0 (0%)	1 (14%)	4 (57%)
Poorly differentiated chordoma ($n = 3$)	3 (100%)	0 (0%)	3 (100%)

Case 3

74 year old Female with fatigue and back pain, followed by voice changes.

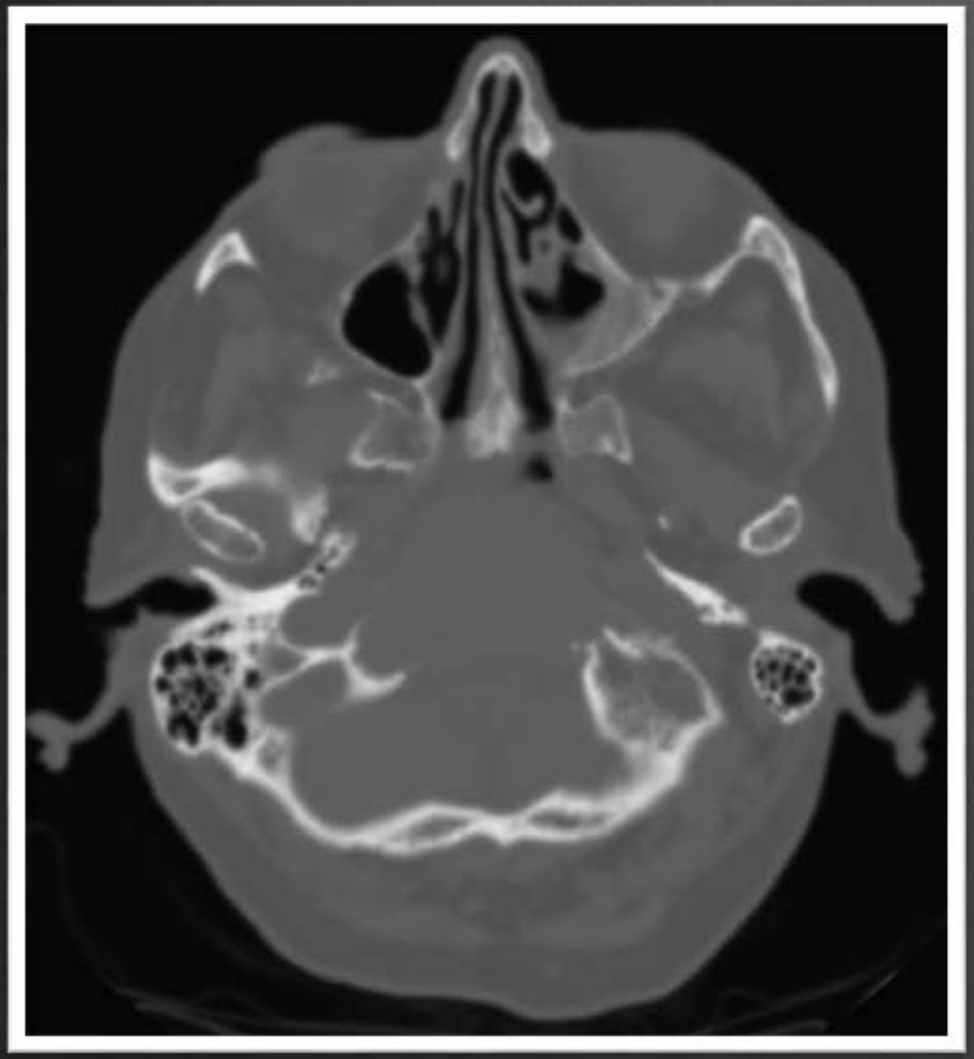

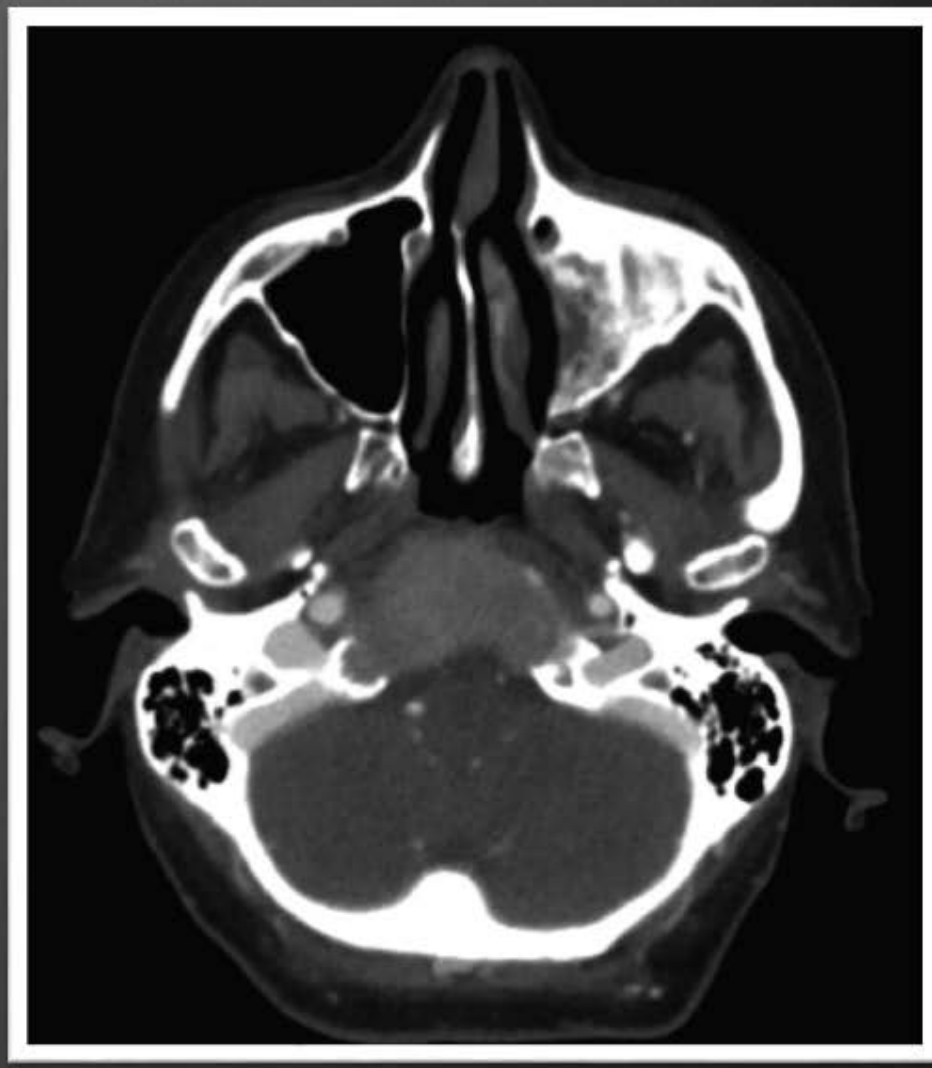

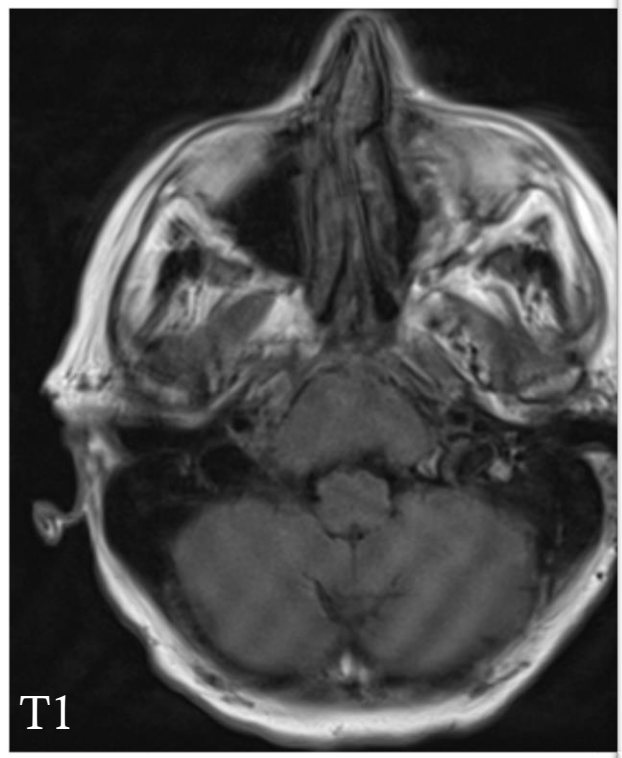
T1

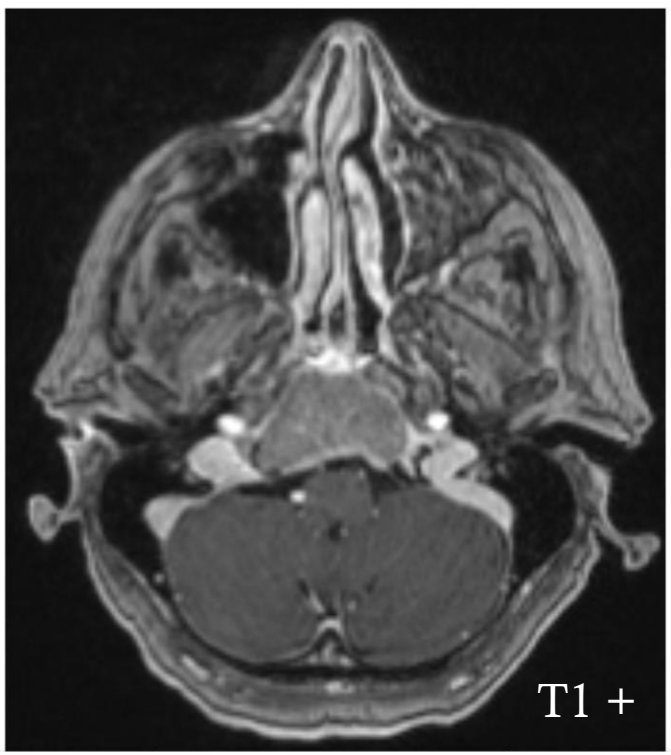
T1 +

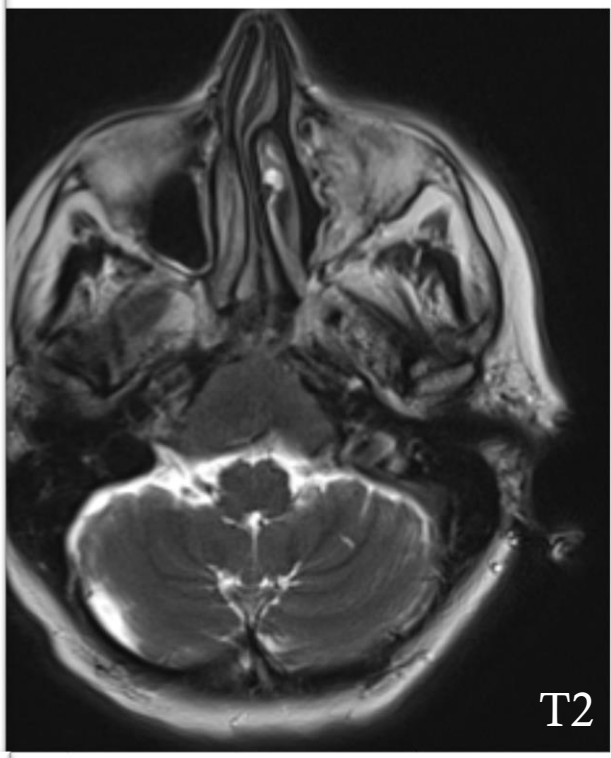
T2

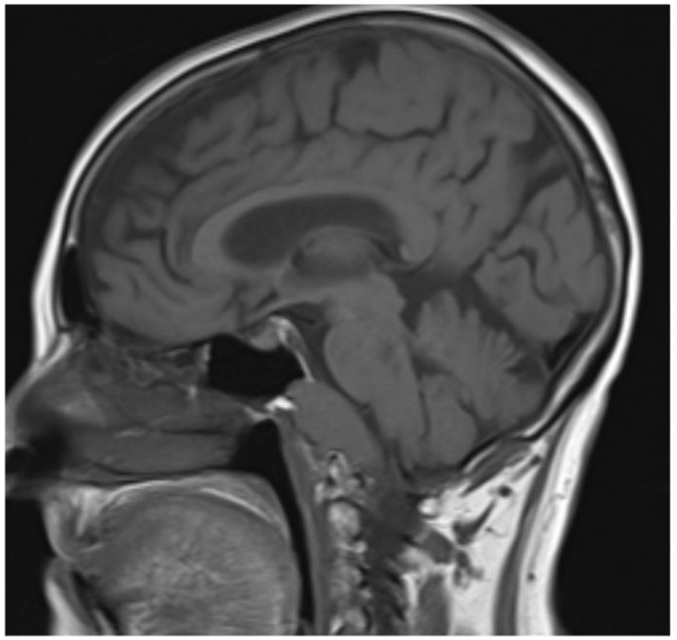

Lesions of Clivus

- Chondrosarcoma
- Chordoma
- Meningioma
- Plasmacytoma
- Metastasis
- Lymphoma
- Langerhans Histiocytosis
- Fibrous Dysplasia
- Infection

Pathology

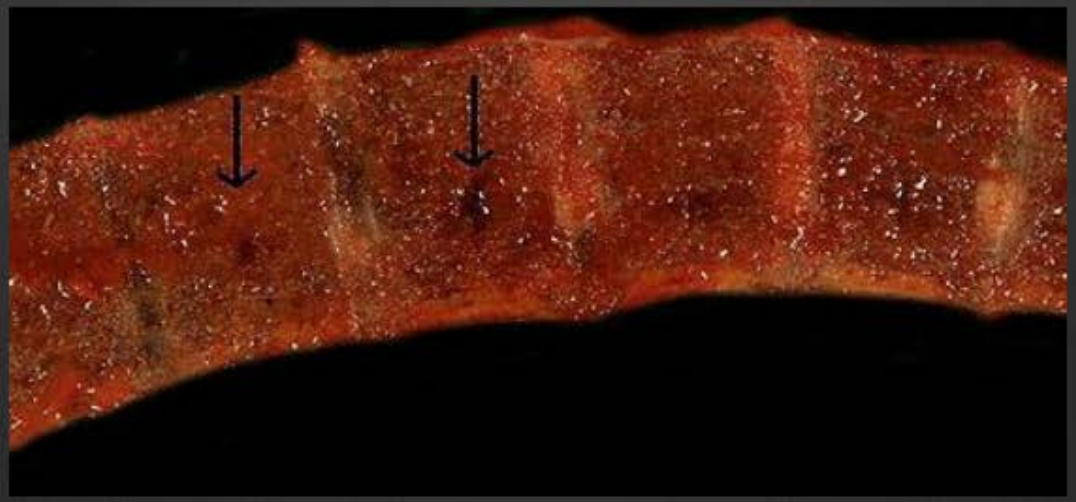

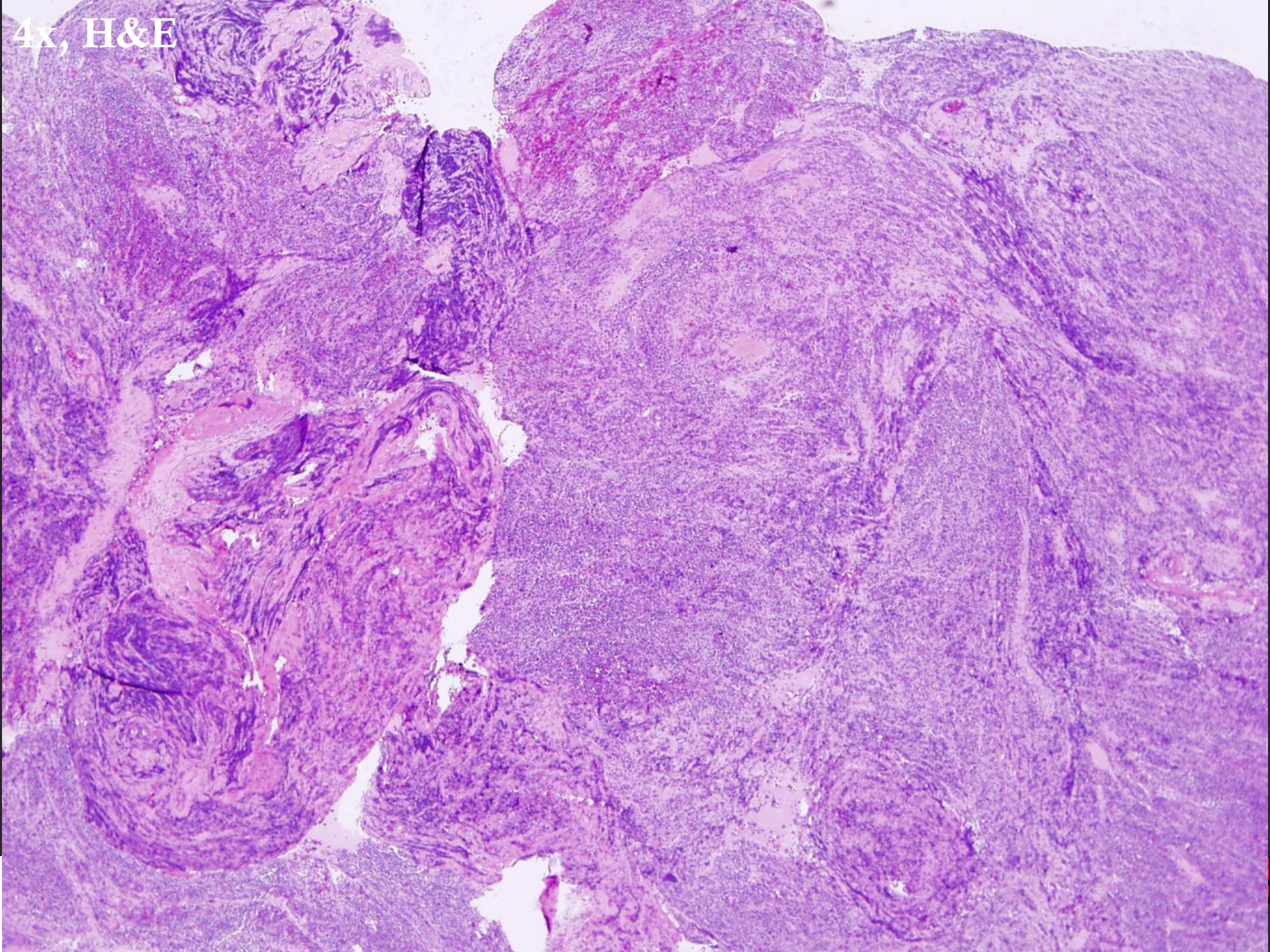
4x, H&E

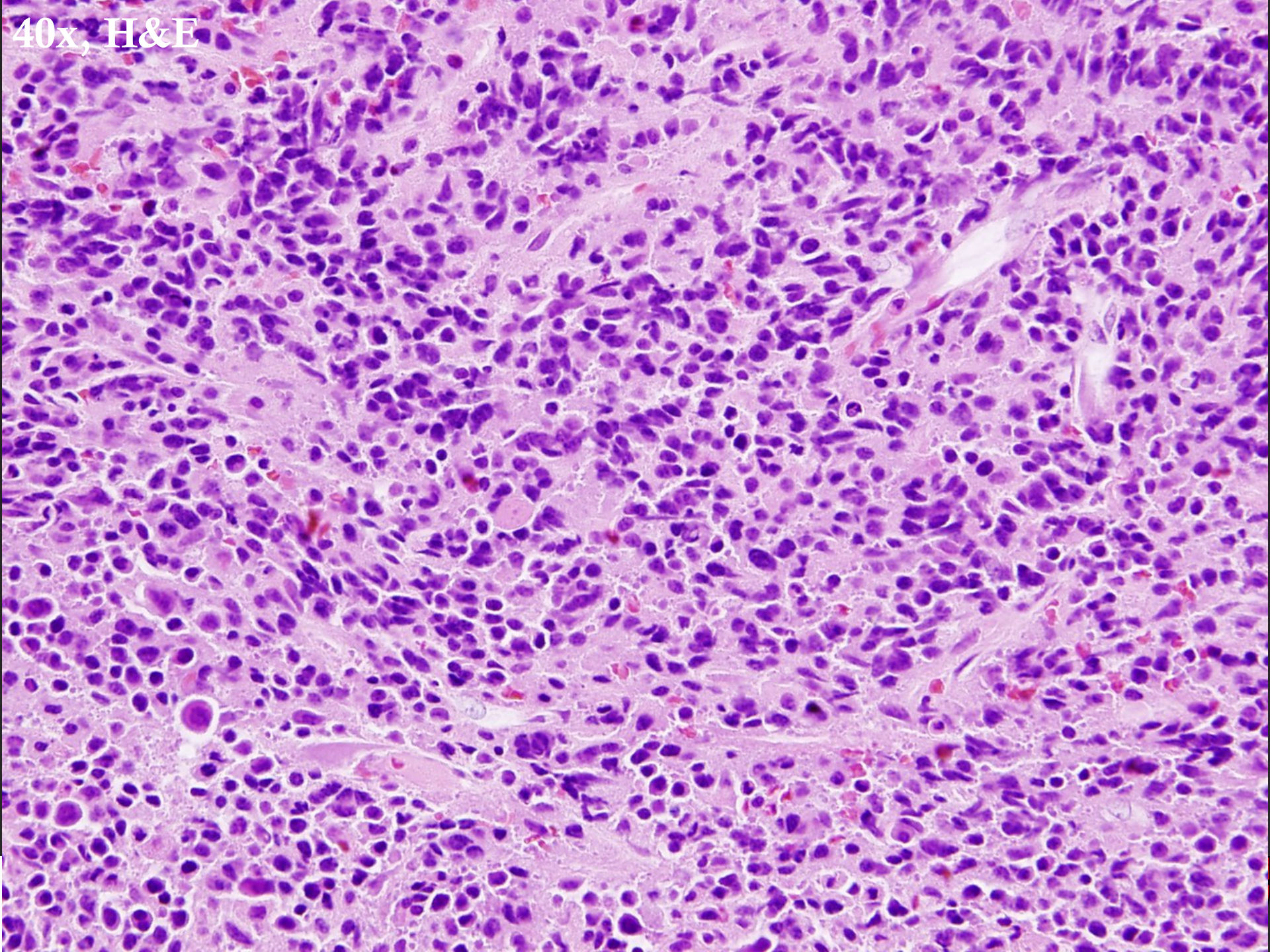
40x, H&E

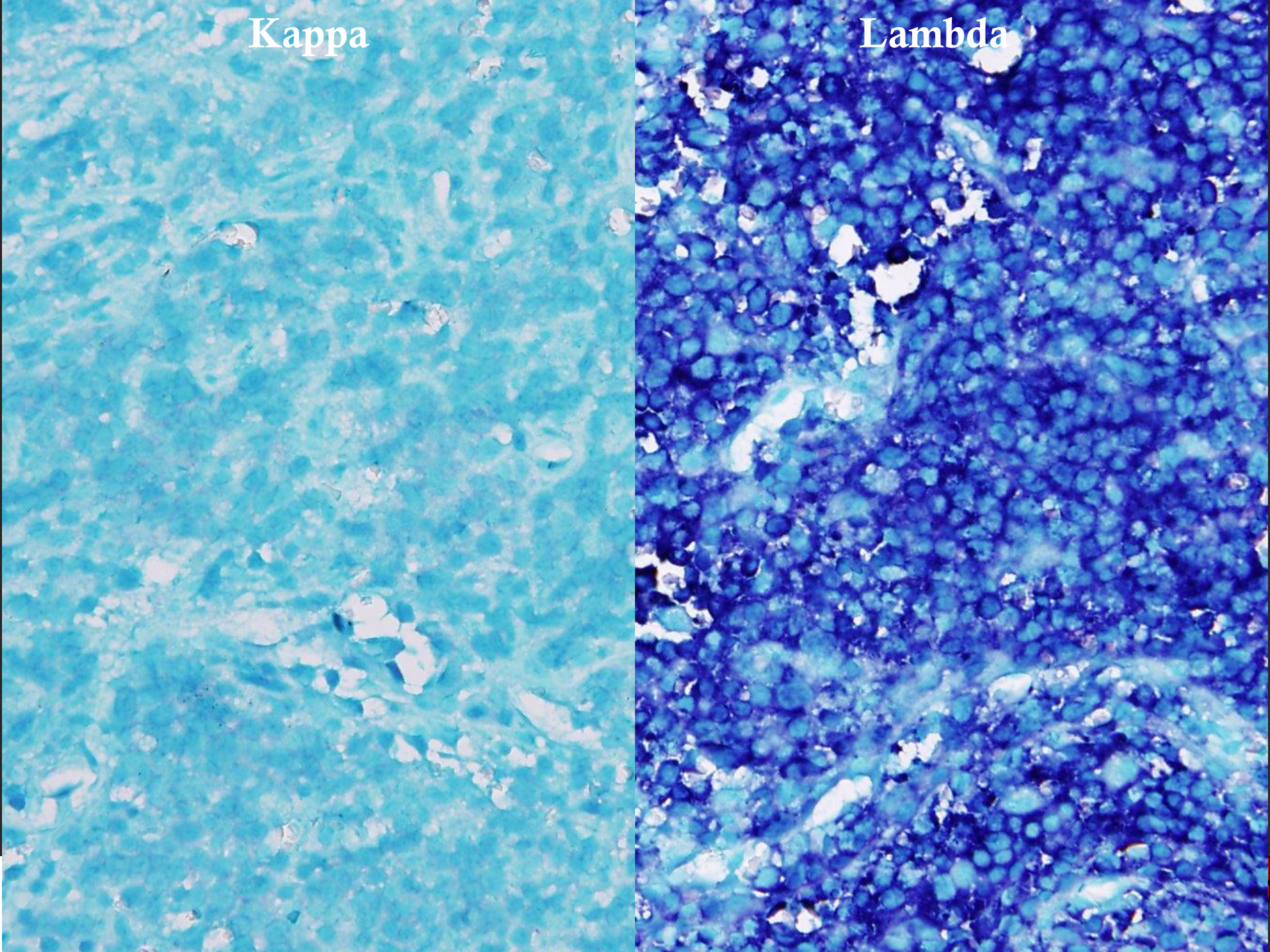
Kappa
Lambda

Final Pathologic Diagnosis

- **PLASMA CELL NEOPLASM (multiple myeloma)**
  - **Cytogenetics:**
    - t(11;14) -> CyclinD1 – IgH fusion
    - Most common translocation in MM (also present in MCL)
  - **Paraproteins:**
    - No serum M spike
    - No urine free light chains

Multiple Myeloma

Radiology

Review

Edgardo J. C. Angtuaco, MD
Athanasios B. T. Fassas, MD
Ronald Walker, MD
Rajesh Sethi, MD
Bart Barlogie, MD

Index terms:
Bone marrow, diseases, 48.3452
Bones, CT, 48.12111
Bones, MR, 48.121411, 48.121412,

Multiple Myeloma: Clinical Review and Diagnostic Imaging[1]

Multiple myeloma (MM) is a malignant clonal neoplasm of plasma cells of B-lymphocyte origin that commonly results in overproduction of large amounts of monoclonal immunoglobulins. Important advances in the therapeutic management

Multiple Myeloma

- Estimates suggest 50% destruction must occur before radiographic demonstration
- 75% of MM patients will have positive findings
- Four forms of involvement
  - Plasmacytoma
  - Diffuse skeletal involvement (myelomatosis)
  - Diffuse skeletal osteopenia
  - Sclerosing myeloma

12 • Radiology • April 2004 Angtuaco et al

TABLE 1
Durie-Salmon Staging System for MM

Stage and Criteria	Value*
I: Low tumor burden†	
Hemoglobin level	>10 g/dL (100 g/L)
Serum calcium level	<12 mg/dL (3 mmol/L)
Radiograph	No bone destruction, or solitary plasmacytoma
Low paraprotein level	
Serum IgG	<5 g/dL (0.05 g/L)
Serum IgA	<3 g/dL (0.03 g/L)
Urine light chain	<4 g/24 h
II: Intermediate tumor burden	
All criteria	Between values for stage I and values for stage III
III: High tumor burden‡	
Hemoglobin level	<8.5 g/dL (85 g/L)
Serum calcium level	>12 mg/dL (3 mmol/L)
Radiograph	More than two advanced lytic lesions
High paraprotein level	
Serum IgG	>7 g/dL (0.07 g/L)
Serum IgA	>5 g/dL (0.05 g/L)
Urine light chain	>12 g/24 h
Associated renal involvement	
A: serum creatinine level	<2 mg/dL (177 μmol/L)
B: serum creatinine level	>2 mg/dL

* Value in parentheses is in SI unit.
† All criteria must be satisfied.
‡ Any criterion must be satisfied.

TABLE 2
Patterns of Normal Signal Intensity on T1-weighted MR Images of Spine in Different Age Groups

Pattern and Site	Age Distribution
1: Hypointense	
Cervical	92% <40 y
Thoracic	70% <30 y
Lumbar	99% <30 y
2: Hypointense with bandlike and triangular hyperintensity at endplates	
Cervical	87% >40 y
Thoracic	88% >50 y
Lumbar	86% >40 y
3: Hyperintense*	
Cervical	75% >50 y
Thoracic	Uniform
Lumbar	76% >40 y

* Pattern 3a is homogeneous; pattern 3b is heterogeneous.

Plasmacytoma

- Lytic lesion that effects the spine, pelvis, skull, ribs, sternum, and proximal appendages
- T1 hypointense area within a generally hyperintense background
- T2 hyperintense area within a generally hypointense background
- Enhance

Case 4

82 year old Female with diplopia


T2

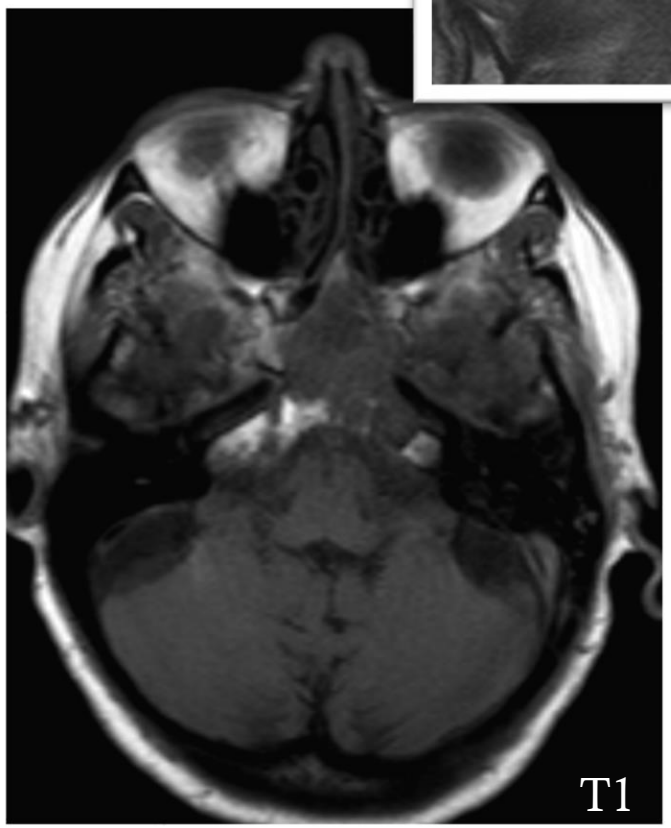
T1

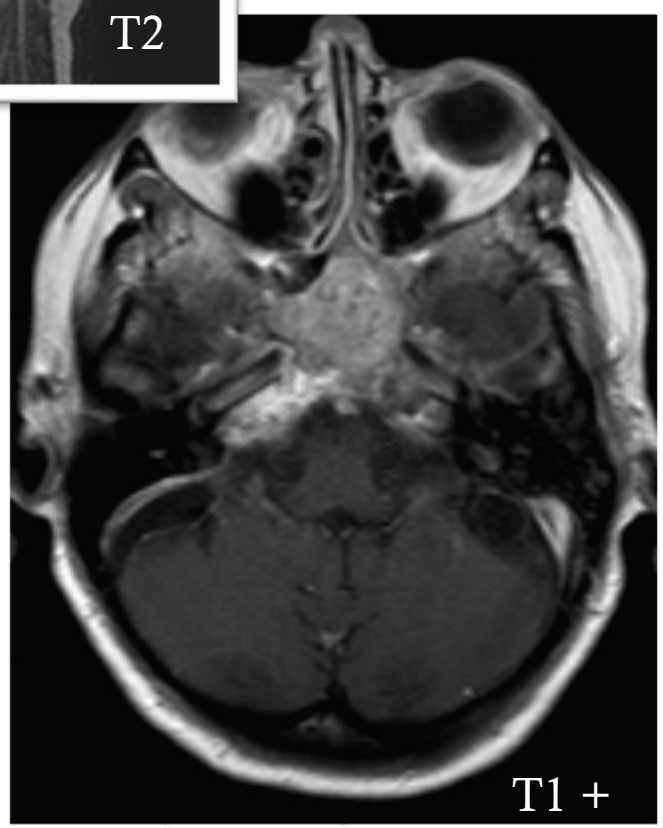
T1 +

Lesions of Clivus

- Chondrosarcoma
- Chordoma
- Meningioma
- Plasmacytoma
- Metastasis
- Lymphoma
- Langerhans Histiocytosis
- Fibrous Dysplasia
- Infection

Pathology

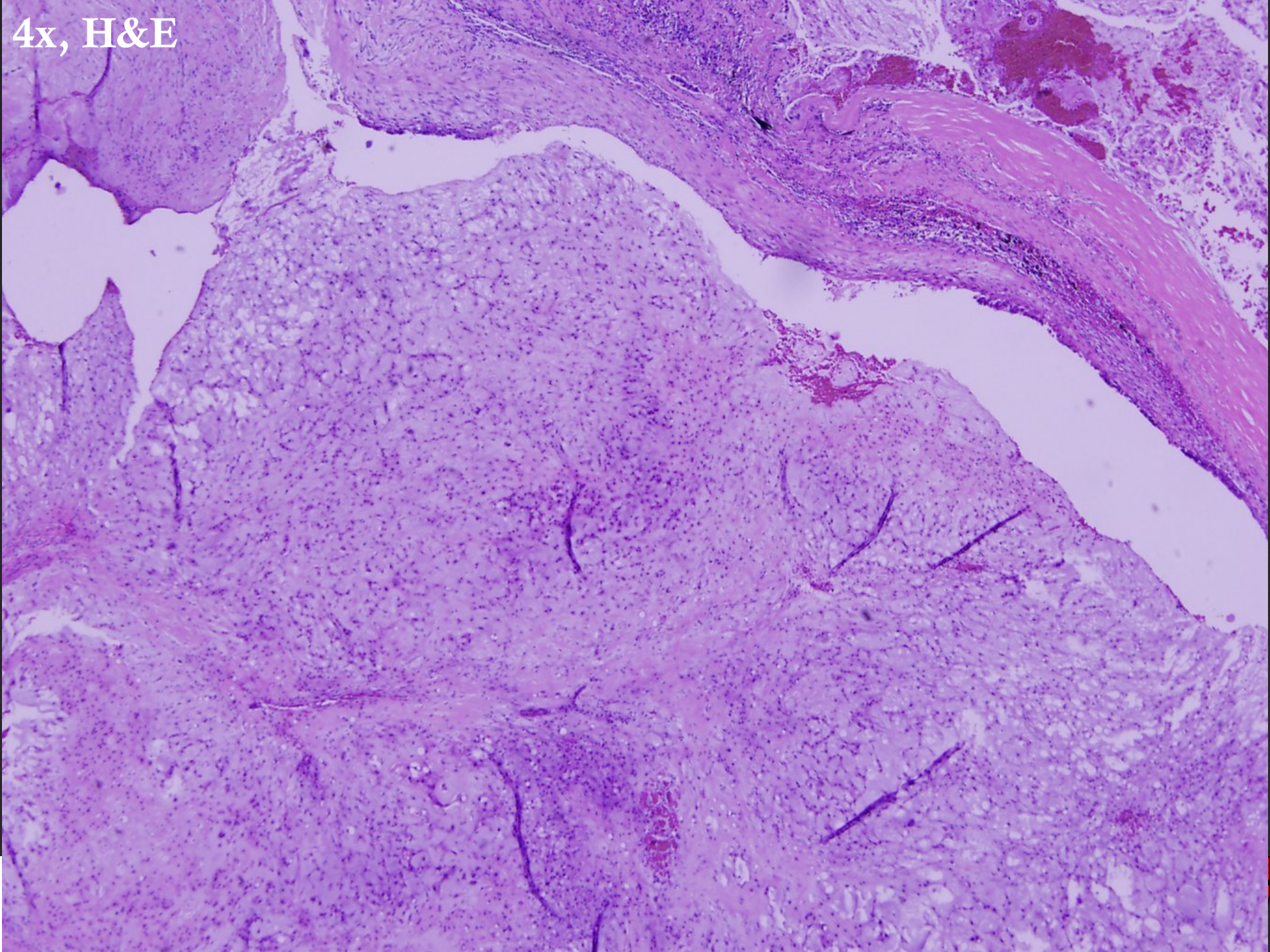
4x, H&E

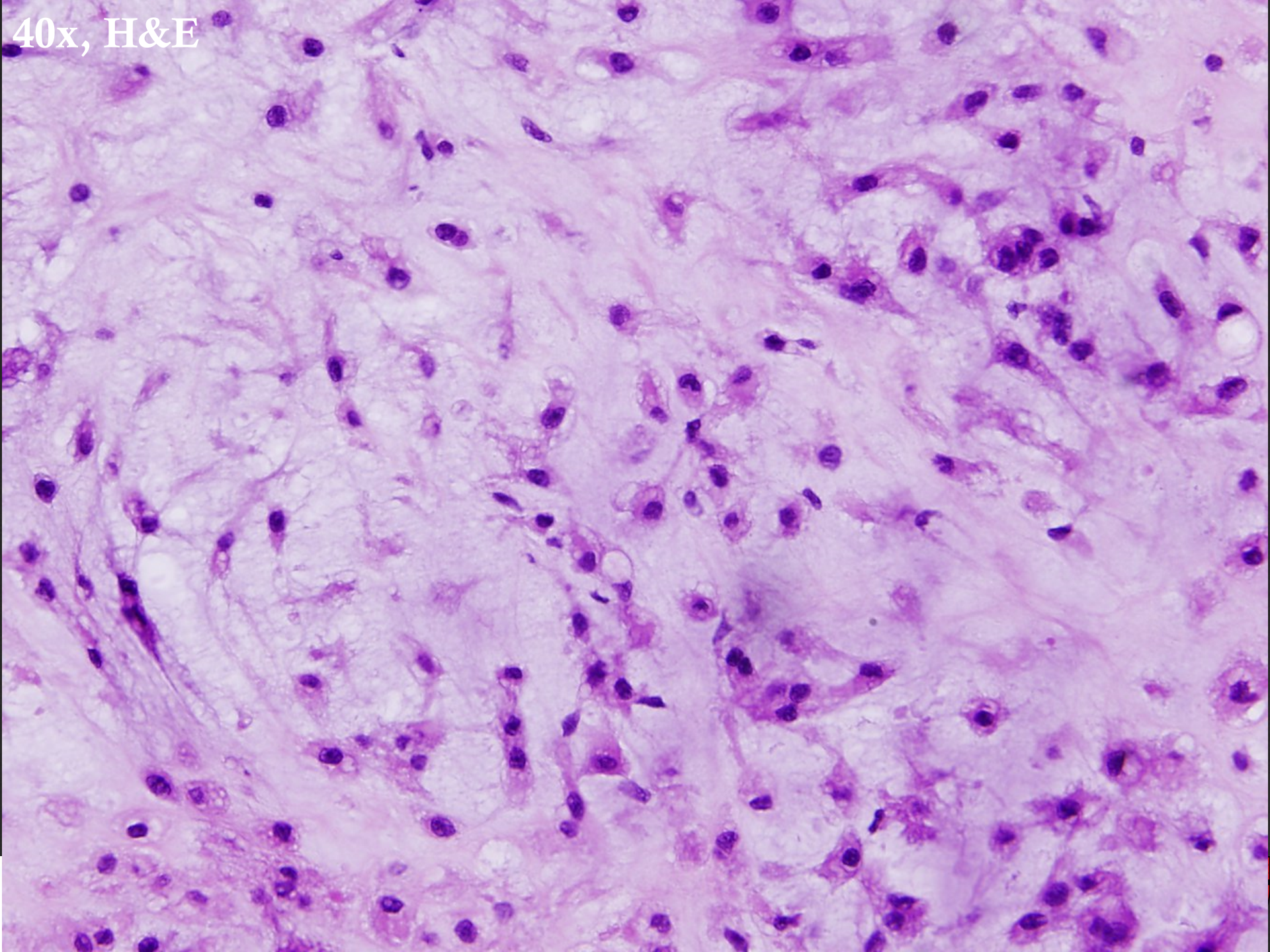
40x, H&E

EMA

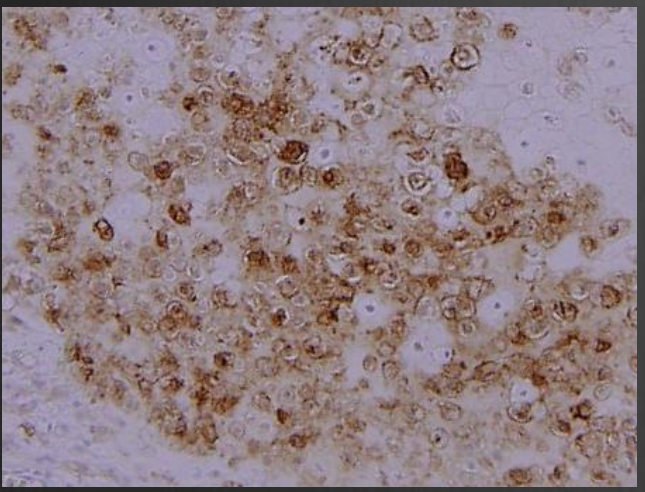

AE1/AE3

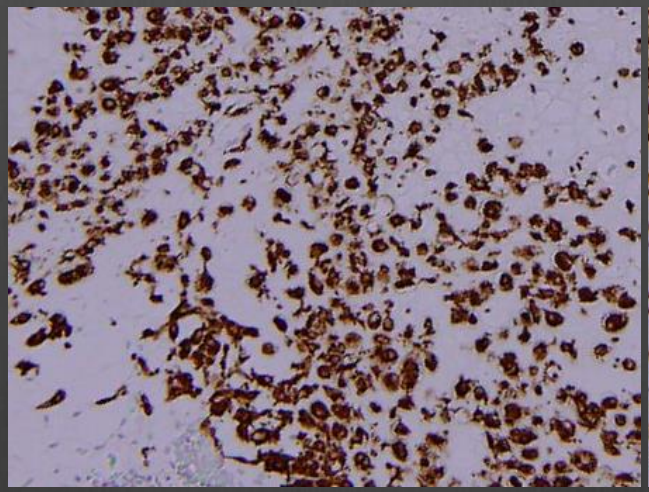

S100

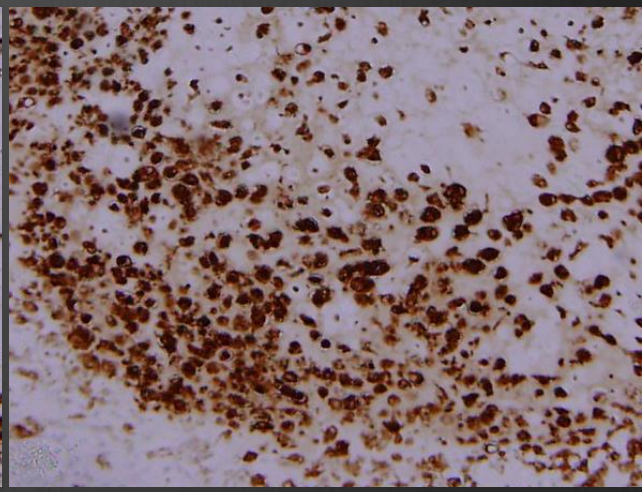

Final Pathologic Diagnosis

- **CHORDOMA**
  - POS: EMA, AE1/AE3, S-100, Brachyury
  - NEG: GFAP

Chordoma

- Embryologic remnant of notochord, entrapped within bone
- Any age, peak prevalence in 4th decade, M:F 2:1, Caucasian
- Distribution: Roughly even across 3 locations

Intracranial

Spinal Cord

Sacral

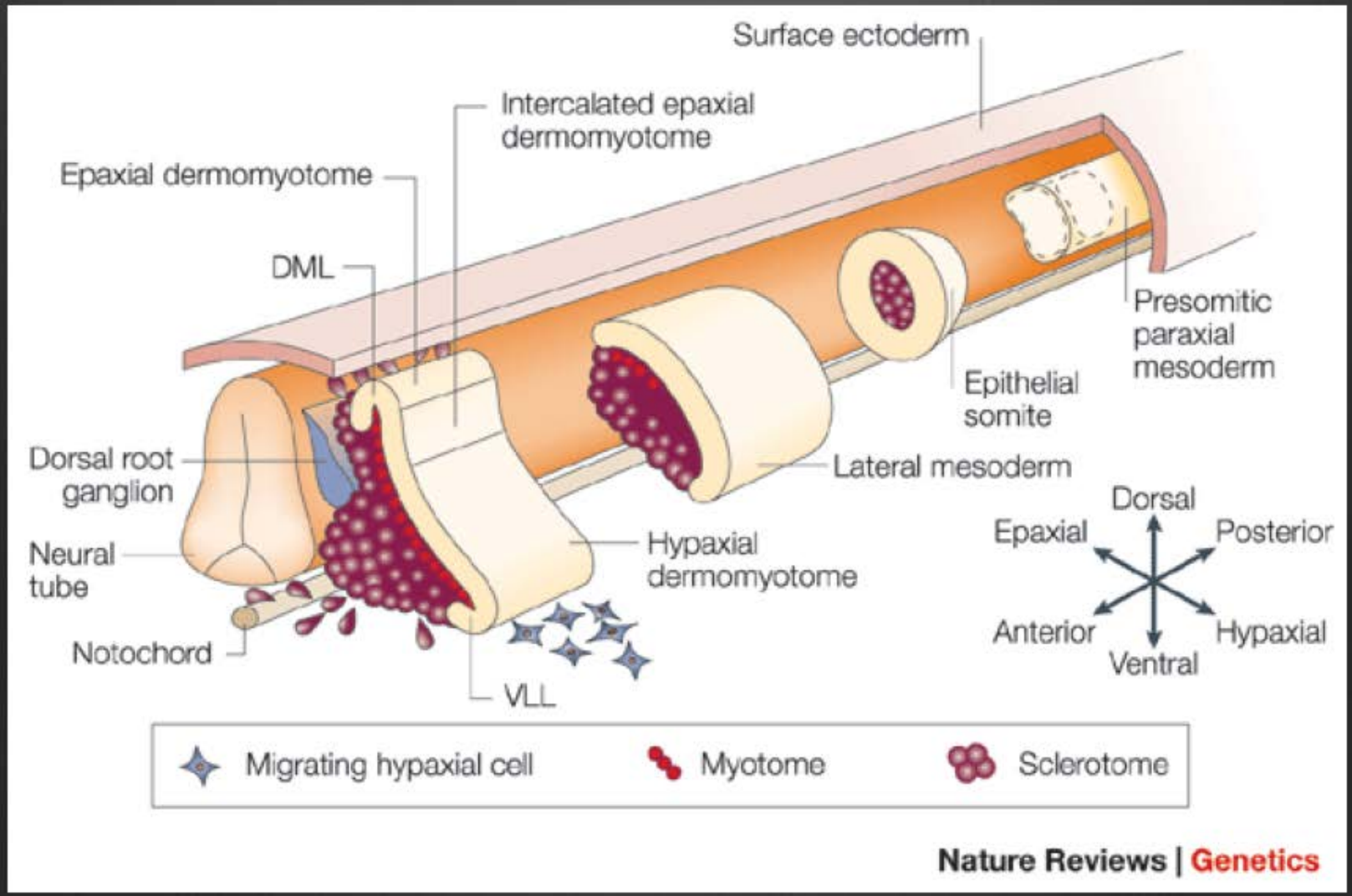
Surface ectoderm
Intercalated epaxial dermomyotome
Epaxial dermomyotome
DML
Presomitic paraxial mesoderm
Epithelial somite
Dorsal root ganglion
Lateral mesoderm
Neural tube
Hypaxial dermomyotome
Notochord
VLL
Dorsal
Epaxial
Posterior
Anterior
Hypaxial
Ventral
Migrating hypaxial cell
Myotome
Sclerotome
Nature Reviews | Genetics

Chordoma

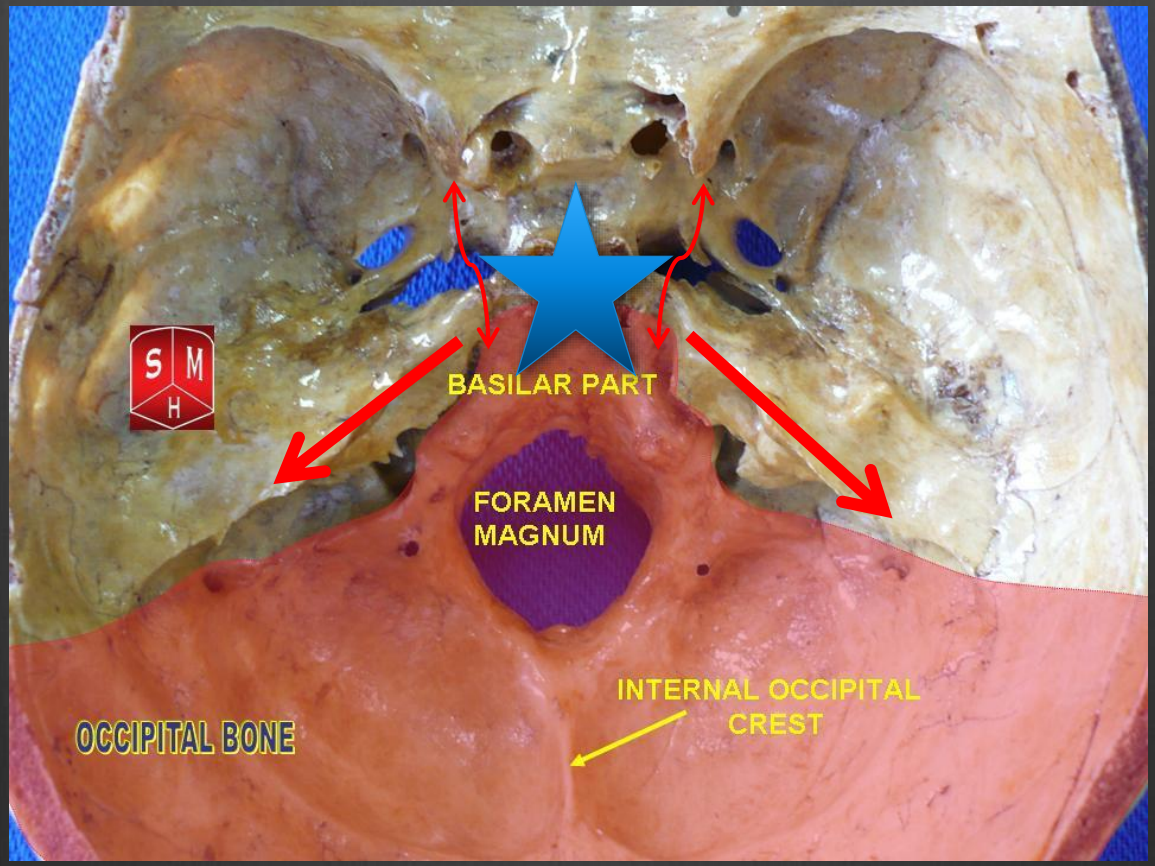
BASILAR PART
FORAMEN MAGNUM
INTERNAL OCCIPITAL CREST
OCCIPITAL BONE

	Chondrosarcoma	Chordoma
CT	Rings and Arcs Linear Globular *Myxoid subtype	Well-circumscribed Variably Hyperattenuating Extensive lytic destruction *Chondriod subtype
T1 (rel. to WM)	Intermediate to Low	Intermediate to Low
T2 (rel. to WM)	Hyperintense	Hyperintense
Enhancement	+, heterogeneous	+, heterogeneous
Behavior	Less Common Majority arise from petro-occipital fissure Better prognosis	More common Midline typically Local Recurrence common Metastasis Rare

DWI: Hot of the Press

Diffusion-Wei…ase Chordoma

…ndrosarcoma

K.W. Yeom, …B. Edwards, and N.J. Fischbein

RESULTS: Chondrosarcoma was a…) and was significantly different from classic chordoma (1474 ± 11… 10^{-6} mm^2/s) ($P < .001$). Poorly differentiated chordoma was char… IR imaging features of enhancement and/or lesion location did n…

CONCLUSIONS: Diffusion-weigh… differentiating chordoma from chondrosarcoma. A prospective s… C in predicting histopathologic diagnosis.

Table 2: ADC values for each tumor type (10^{-6} mm^2/s)

Tumor	Mean ADC (Median)	Minimum ADC (Median)	Maximum ADC (Median)
Chondrosarcoma ($n = 9$)	2051 ± 262 (1977)	1488 ± 360 (1352)	2503 ± 512 (2392)
Classic Chordoma ($n = 7$)	1474 ± 117 (1460)	905 ± 118 (860)	2199 ± 255 (2217)
Poorly Differentiated Chordoma ($n = 3$)	875 ± 100 (871)	491 ± 210 (469)	1503 ± 127 (1557)

Table 3: MRI features for each tumor type

Tumor	T2 Hypointensity	>90% Enhancement	Clival Location
Chondrosarcoma ($n = 9$)	0 (0%)	5 (56%)	4 (44%)
Classic chordoma ($n = 7$)	0 (0%)	1 (14%)	4 (57%)
Poorly differentiated chordoma ($n = 3$)	3 (100%)	0 (0%)	3 (100%)

Chordoma

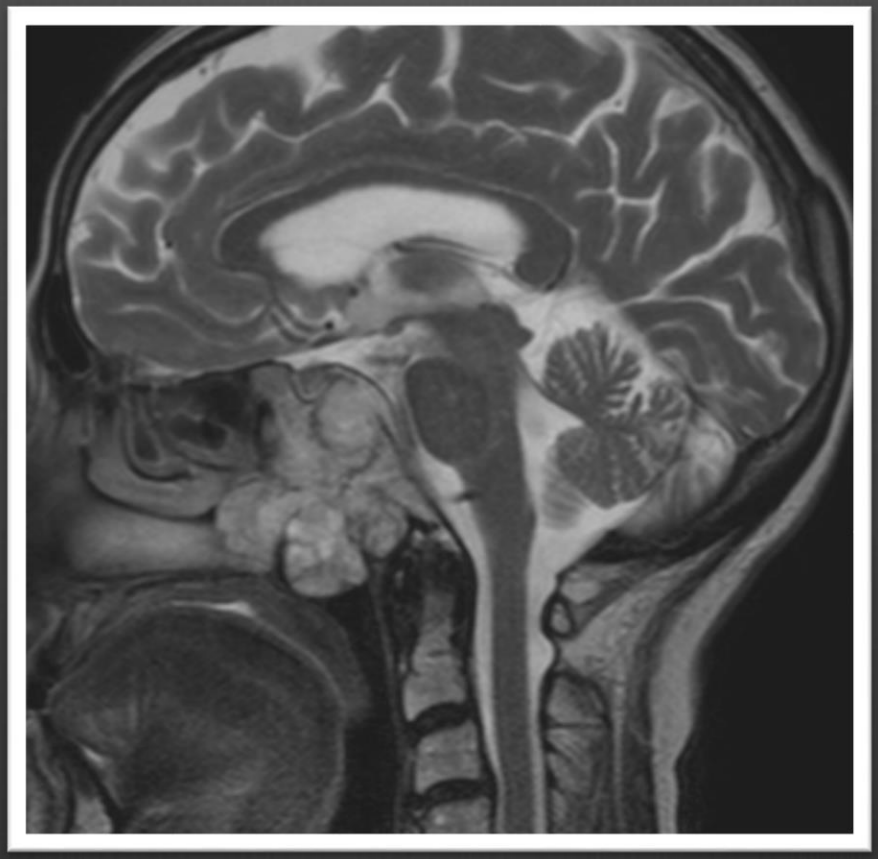

Low signal intensity septations that separate high signal intensity lobules commonly seen

Chordoma

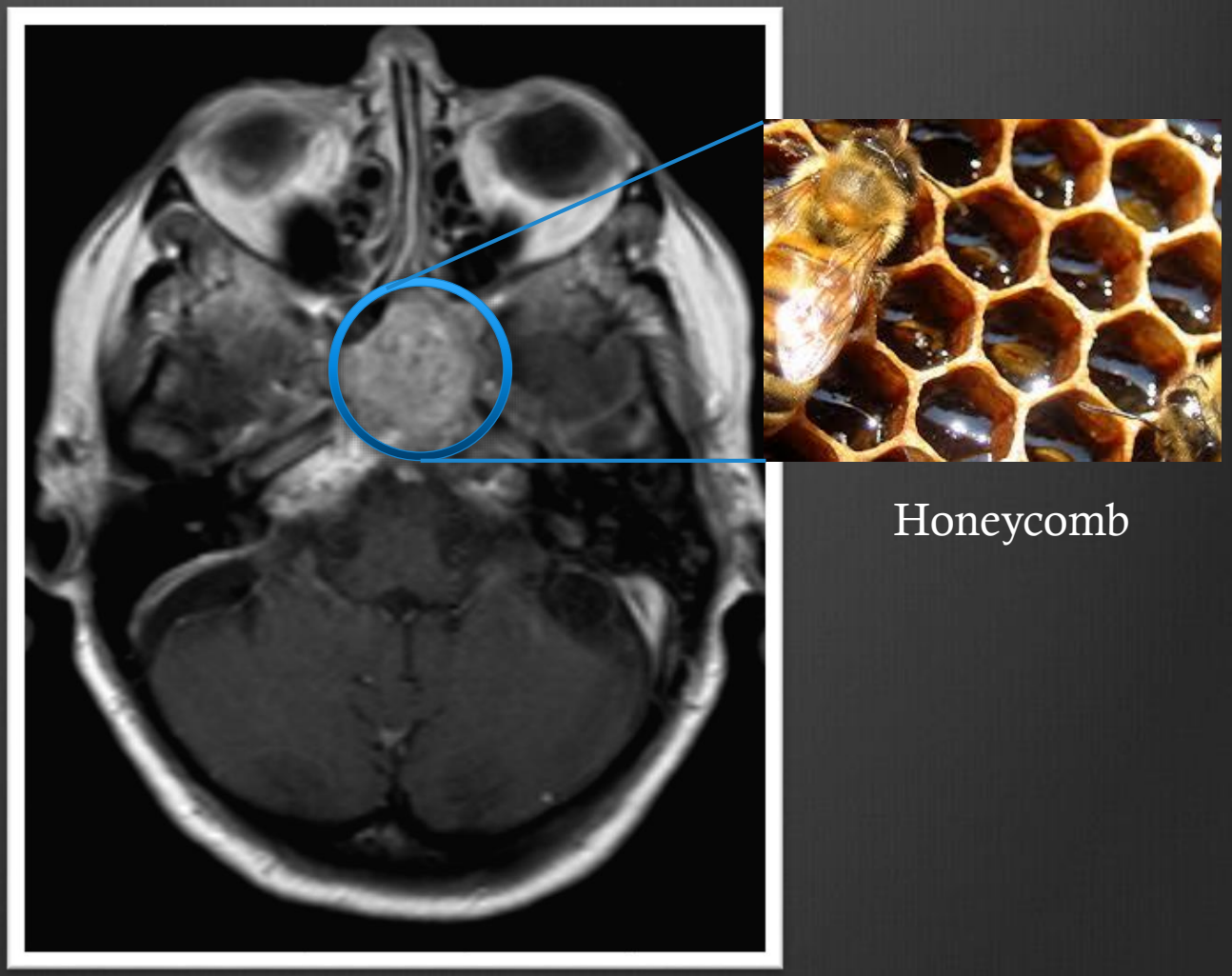

Honeycomb

Post contrast, may see low signal areas of non-enhancement, reflecting necrosis or mucin

Chordoma

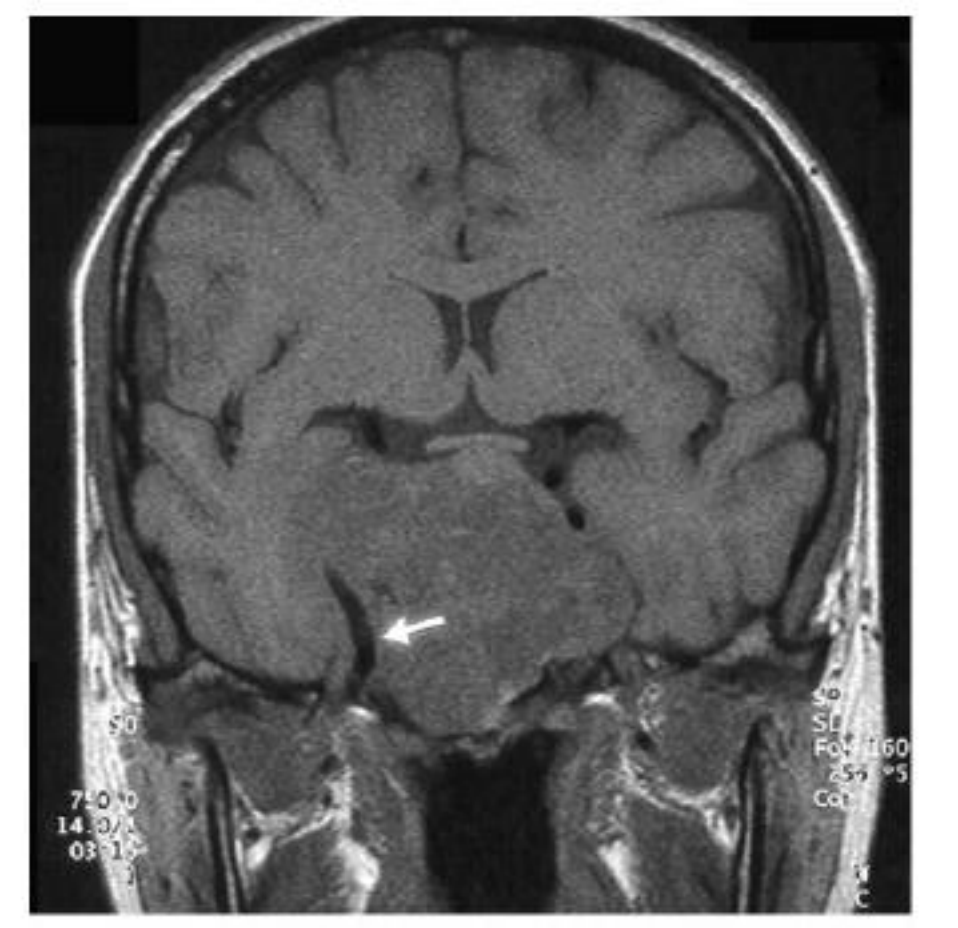

Vascular displacement common, narrowing rare

Chordoma: Behavior

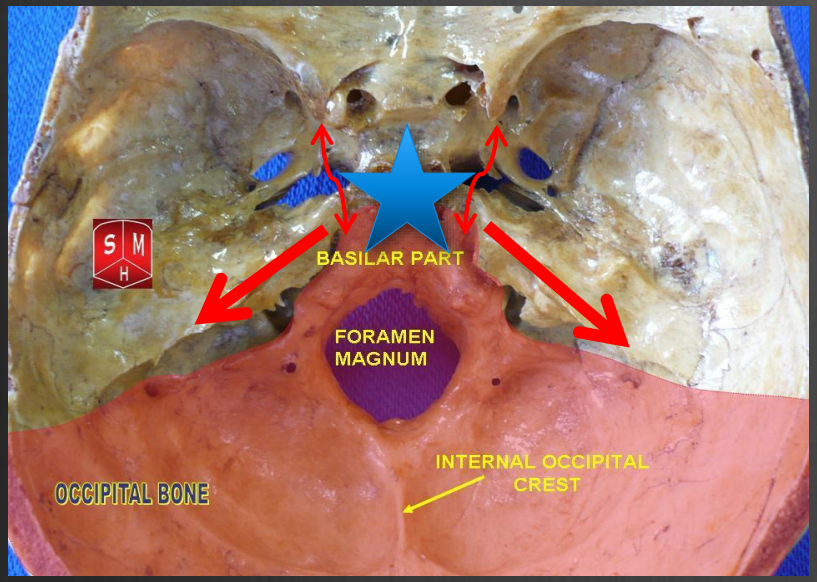

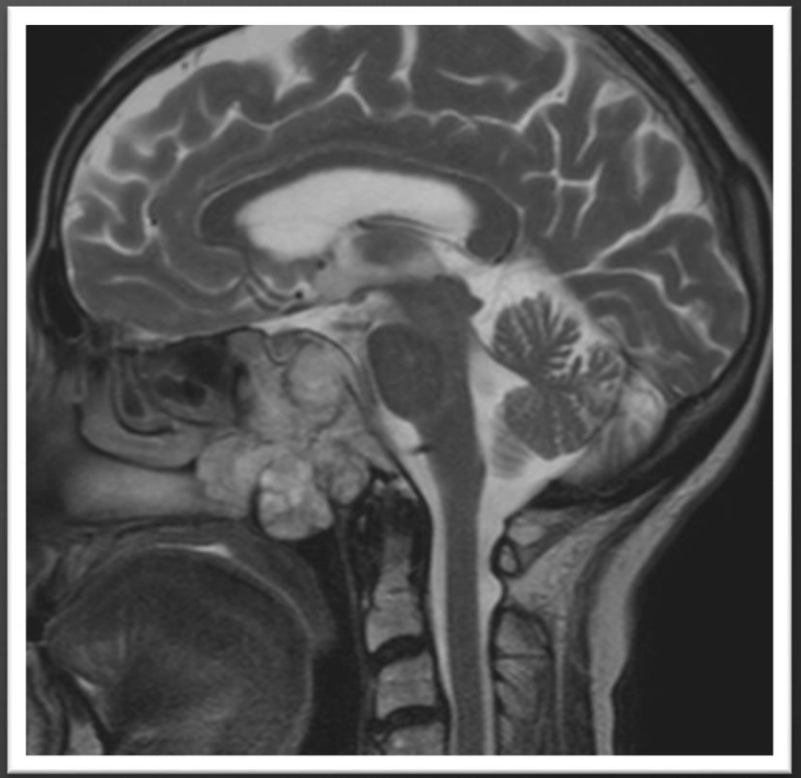

Treated with resection followed by proton beam radiation
Local recurrence common; Metastasis rare

The End